

PLASTICITY OF MAGNESIUM CRYSTALS

by

Bud Caesar Wonsiewicz

S.B. Massachusetts Institute of Technology
(1963)

Submitted in Partial Fulfillment of the

Requirements for the Degree of

DOCTOR OF PHILOSOPHY

at the

Massachusetts Institute of Technology

June 1966

Signature of Author
Department of Metallurgy

Signature of Professor
in Charge of Research

Signature of Chairman of
Departmental Committee on
Graduate Students

PLASTICITY OF MAGNESIUM CRYSTALS

by

Bud Caesar Wonsiewicz

Submitted to the Department of Metallurgy on February 11, 1966
in partial fulfillment of the requirements for the
Degree of Doctor of Philosophy

ABSTRACT

The plasticity transition in magnesium was studied in plane-strain compression of single crystals and polycrystalline material from room temperature to 307°C. Reduction of single crystals along the c-axis was accommodated by twinning on $\{10\bar{1}1\}$ and retwinning on $\{10\bar{1}2\}$, followed by basal shear in the doubly twinned volume. Deformation in that mode can result in sufficient independent shears for arbitrary shape change. Fracture in c-axis compression, below about 100°C, has been related to excessive shear caused by unloading from the stress for $\{10\bar{1}1\}$ twinning (~ 50 ksi at 20°C) to that for slip within the twin (~ 3 ksi); ductility follows from heating because the stress difference is lowered and the twin volume, in which elastic strain energy is dissipated on unloading, is increased. The stress for $\{10\bar{1}1\}$ twinning is strongly temperature dependent but not given by a critical resolved shear-stress law. The latter is attributed to the influence of stress concentration from prior intersecting shear on nonbasal planes, the former to the temperature dependence of that preliminary slip.

Thesis Supervisor: Walter A. Backofen

Title: Professor of Metallurgy

TABLE OF CONTENTS

	<u>Page</u>
ABSTRACT-----	ii
LIST OF ILLUSTRATIONS-----	v
LIST OF TABLES-----	viii
ACKNOWLEDGMENTS-----	ix
INTRODUCTION-----	1
EXPERIMENTAL PROCEDURES-----	6
Specimen Preparation-----	6
Testing-----	6
Analysis of Data-----	9
Metallographic Examination-----	9
RESULTS-----	10
Compression Parallel to the c-axis-----	10
Room Temperature-----	10
Elevated Temperature-----	17
Polycrystalline Material-----	20
Compression Perpendicular to c-axis-----	20
Room Temperature-----	25
Elevated Temperature-----	30

	<u>Page</u>
DISCUSSION-----	31
$\{10\bar{1}1\}$ Twinning-----	31
Plasticity Transition-----	36
SUMMARY AND CONCLUSIONS-----	36
REFERENCES-----	37
APPENDIX 1 - EXPERIMENTAL DETAILS-----	39
APPENDIX 2 - CALCULATION OF LINEAR HARDENING RATE DUE TO ELASTIC EFFECTS IN CHANNEL-----	46
APPENDIX 3 - CALCULATION OF RESOLVED SHEAR STRESS FOR $\{10\bar{1}1\} \langle 10\bar{1}2 \rangle$ TWINNING-----	49
APPENDIX 4 - PROOF THAT A $(01\bar{1}1)$ PLANE IN THE MATRIX IS NEARLY PARALLEL TO A $\{01\bar{1}1\}$ PLANE WITHIN A $(10\bar{1}2)$ TWIN-----	51
SUGGESTIONS FOR FUTURE RESEARCH-----	54
BIOGRAPHICAL NOTE-----	57

LIST OF ILLUSTRATIONS

<u>Figure</u>		<u>Page</u>
1	Some Details of Twinning in Magnesium. (a) Twinning on $\{10\bar{1}2\}$ occurs in tension perpendicular or compression parallel to the (0001) basal plane and reorients the basal plane through 86.3° . (b) Under an opposite system of loading $\{10\bar{1}1\}$ twin can form and then retwin (c) on $\{10\bar{1}2\}$. A similar double twinning process (d-e) can occur on a $\{10\bar{1}3\}$ plane.-----	3
2	Proposed Compression Experiments (a) Parallel to the [0001] c-axis with expansion limited to $[11\bar{2}0]$; it might be expected that slip or twinning on planes of the form $\{11\bar{2}x\}$ would be favored. (b) Parallel to [0001] with expansion limited to $[10\bar{1}0]$; now slip or twinning on planes of the form $\{10\bar{1}x\}$ might be favored. (c) Normal to [0001] but without expansion along that axis; pyramidal or prismatic $\{10\bar{1}0\}$ slip ought to be encouraged since the basal plane is unstressed and $\{10\bar{1}2\}$ twinning must lead to an expansion in the direction of restraint.---	5
3	Schematic Arrangement of Crystal, Indentor and Channel for Enforcing Plane Strain. The adjustable jaw restricts lateral spreading during compression and is supported by 3-1/4 x 20 hardened cap screws.-----	8
4	True-stress:true-strain Curves for Magnesium Crystals Compressed Along the [0001] c-axis with Expansion Limited to $[1\bar{2}10]$.-----	11
5	True-stress:true-strain Curves for Magnesium Crystals Compressed Along the [0001] c-axis with Expansion Limited to $[10\bar{1}0]$.-----	12
6	Recrystallization in a Doubly Twinned Band Along $\{10\bar{1}1\}$ formed at Room Temperature. This observation made a month after deformation, although recrystallization was apparent in examination within one-half hour. 500X under polarized light. Plane of view \sim (0001). Etched in acetic picral.--	15

<u>Figure</u>		<u>Page</u>
7	Fracture Near the Indentor Edge in c-axis Compression at Room Temperature.	
	(a) Cracking along $\{10\bar{1}1\}$ at a prepolished surface. Unetched 100X.	
	(b) Cracking along $\{10\bar{1}1\}$ exclusively; surface curves in prepolishing. Unetched 100X.-----	16
8	Twinning at Elevated Temperatures in Magnesium Crystals Compressed Along $[0001]$. 40X, under polarized light. Etched in acetic picral.	
	(a) 200°C; $\{10\bar{1}1\}$ bands are recrystallized, $\{10\bar{1}3\}$ are not. Dark, horizontal $\{10\bar{1}2\}$ twins formed on unloading.	
	(b) 272°C; $\{10\bar{1}1\}$ recrystallized bands.-----	18
9	Maximum Stress σ_{\max} versus Temperature. Dashed line σ_b indicates an estimate of normal stress for basal slip within a $\{10\bar{1}1\}$ twin in c-axis compression. Full lines represent experimental data for compression along stated directions.-----	19
10	Rotation of $\{10\bar{1}1\}$ Bands During 40% Compression Along $[0001]$ at 116°C. Initially, bands at A were near the indenter edge, but were moved out from under the indenter during the test; thus they underwent less than the full deformation and so are still located along $\{10\bar{1}1\}$. With heavier deformation towards the center, bands were rotated away from the loading axis, to make a final angle of about 30° with the basal plane. 40X under polarized light. Etched in acetic picral.-----	21
11	True-stress:true-strain Curves for Plane-strain Compression of Polycrystalline Magnesium.-----	22
12	True-stress:true-strain Curves for Magnesium Crystals Compressed Along $[10\bar{1}0]$ with Expansion Limited to $[1\bar{2}10]$.--	23
13	True-stress:true-strain Curves for Magnesium Crystals Compressed Along $[1\bar{2}10]$ with Expansion Limited to $[10\bar{1}0]$.--	24

<u>Figure</u>		<u>Page</u>
14	{10 $\bar{1}2$ } Twins and {10 $\bar{1}1$ } Doubly Twinned Volumes in Magnesium Crystals After Compression Perpendicular to [0001]. 40X under polarized light. Etched in acetic picral.	
	(a) Compression along [1 $\bar{2}$ 10]. Two different sets of {10 $\bar{1}2$ } twins were formed. Most of the {1011} appeared to penetrate {10 $\bar{1}2$ } twins.	
	(b) Compression along [10 $\bar{1}0$]. Only a single set of {10 $\bar{1}2$ } twins appeared and was penetrated by {1011}.-----	28
1A	Experimental Apparatus	
	(a) Compression fixture and extensometer with channel, specimen and indenter in place.	
	(b) Adjustable channel with specimen and indenter inserted.-----	41
1B	True-stress:true-strain Plane-strain Compression Curves for Single Crystals of Differing Surface Roughness.-----	44

LIST OF TABLES

<u>Table</u>		<u>Page</u>
I	Resolved Shear Stresses for $\{10\bar{1}1\}$ Twinning at Room Temperature-----	14
II	Initial Linear Hardening Rate for Compression Perpendicular to the c-axis-----	26
III	Estimate of Basal Shear Strain in the Twinned Volume-----	34

ACKNOWLEDGMENTS

The author is grateful to Professor W. A. Backofen for the research opportunity and for his patient guidance throughout all phases of the doctorate program. He also wishes to thank Professor W. F. Hosford, Jr. of the University of Michigan for suggesting much of the work, and the students and staff to the Metals Processing Laboratory for helpful discussions and suggestions.

Dr. S. L. Couling of the Dow Metallurgical Laboratory generously supplied the sublimed magnesium and spectrographic analysis.

The research was sponsored by the Atomic Energy Commission.

PLASTICITY OF MAGNESIUM CRYSTALS

INTRODUCTION

The basic symmetry of hexagonal close-packed (HCP) crystals has the effect of limiting the number of independent slip systems and making twinning an important deformation mechanism. The general result in wrought polycrystalline aggregates is a more or less sharply developed texture (or preferred orientation) which underlies a strong anisotropy in mechanical behavior. Knowing how the one influences the other is essential background for the use of such materials.

Magnesium is the oldest structural HCP metal but was of interest to this work because of the unexplained plasticity transition that it undergoes somewhere in the neighborhood of 200°C.^{1,2} At lower temperatures, plastic deformation before fracture in polycrystalline material is limited, while at higher temperatures extensive deformation is possible. The transition temperature commonly determines the lower limit of the range in which magnesium is worked.

The limited ductility can be traced to a lack of independent crystallographic shears. A minimum of five are required for arbitrary shape change.³ Around room temperature, however, slip on all known systems provides only four.⁴ In each case, the slip direction is in the (0001) basal plane so that slip does not allow strain along the c-axis. With

increasing temperature, more slip occurs on the $\{10\bar{1}1\}$ pyramidal plane but without change in direction.¹ Thus, that development alone cannot explain the transition temperature.

Twinning on $\{10\bar{1}2\}$ leads to a small amount of expansion along the c-axis with the basal plane in the twin being reoriented through 86.3° . Therefore, under load that would induce twinning (Fig. 1a) the stress on the basal slip system is not substantially changed, and continued slip within the twins is unlikely to contribute much to the total strain. On the other hand, the effect of $\{10\bar{1}1\}$ twinning is contraction parallel to the c-axis, with the basal plane being rotated through only about 56° (Fig. 1b) under loads that are basically the opposite of those for $\{10\bar{1}2\}$ twinning.

Microscopic bands have been observed in hot-rolled magnesium alloys, oriented at right angles to the rolling direction and inclined to the rolling plane along surfaces that supported high shear stress during reduction; the basal plane was found to lie essentially parallel to the plane of the band. The bands were first believed to result from fracturing and rewelding,⁵ but later work on cold-rollable alloys has given clear indication that they form by a double twinning mechanism.⁶

With reference to the usual texture of rolled sheet, the first step in the over-all mechanism is twinning on $\{10\bar{1}1\}$; then the material in that twin is twinned again on $\{10\bar{1}2\}$. The sequence is indicated in Figs. 1b and 1c, where the basal plane is shown finally to be located

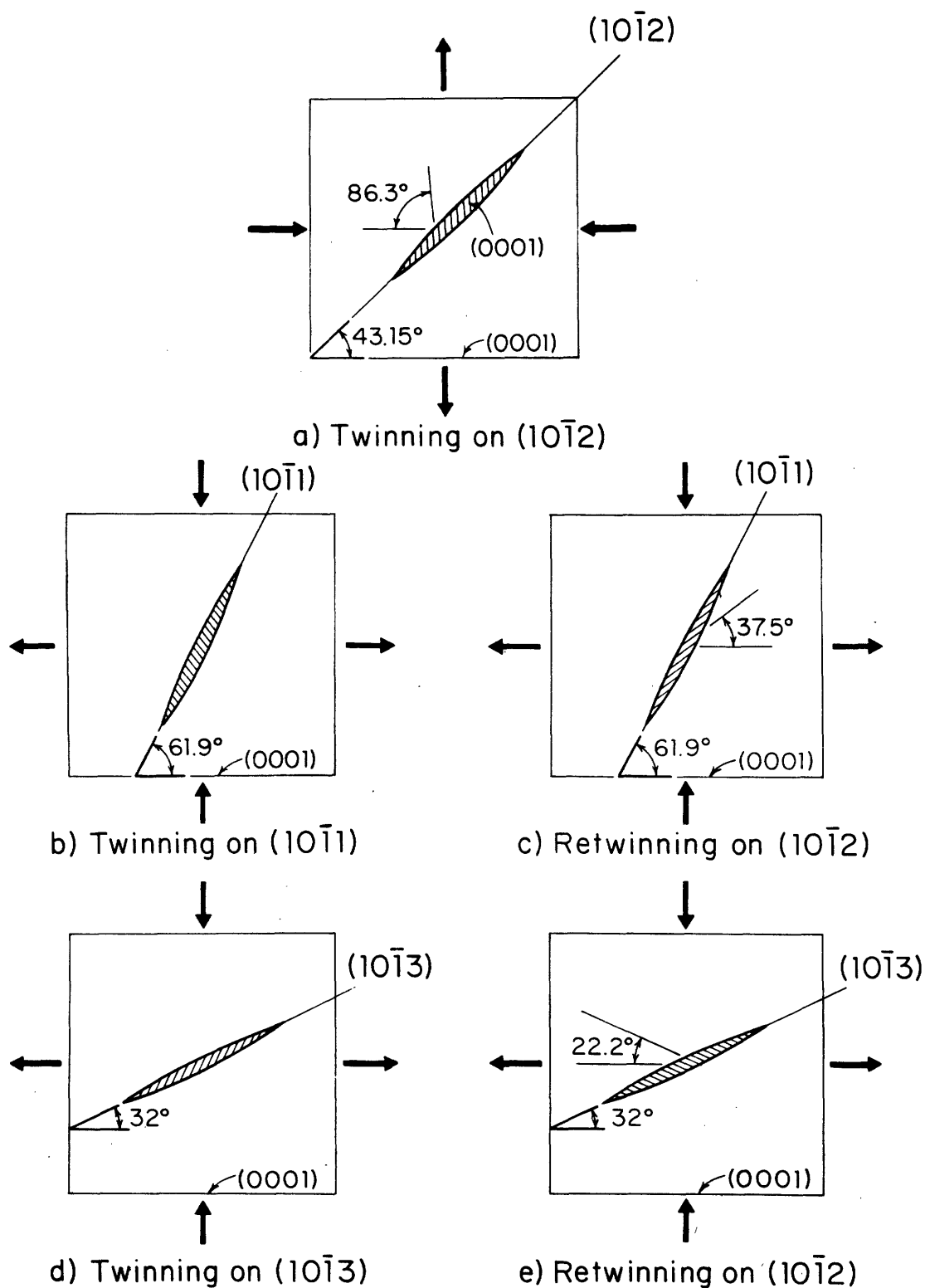


Fig. 1. Some Details of Twinning in Magnesium. (a) Twinning on $\{10\bar{1}2\}$ occurs in tension perpendicular or compression parallel to the (0001) basal plane and reorients the basal plane through 86.3° . (b) Under an opposite system of loading $\{10\bar{1}1\}$ twin can form and then re-twin (c) on $\{10\bar{1}2\}$. A similar double twinning process (d-e) can occur on a $\{10\bar{1}3\}$ plane.

at an angle of 37.5° from its original position in the untwinned matrix. In a similar way it is possible for the first twin to form on $\{10\bar{1}3\}$ with retwinning on $\{10\bar{1}2\}$, as in Figures 1d and 1e.⁷ Both twinning stages in either case lead to contraction along the c-axis. The final point in the argument is that the basal plane is rotated, as it slips, into alignment with the habit plane of the band, and intense basal-plane shear occurs. One indication that such a development is perhaps unique to magnesium is the characteristic tilting of basal-plane poles towards the rolling direction.⁸ In titanium, zirconium, and beryllium, the tilting is in the transverse direction, presumably because of extensive prism slip in those materials.⁹

Although double twinning was recognized, the question not answered when this work was begun was what, if anything, did it have to do with the plasticity transition in magnesium.

It was decided that the most straightforward approach to a study of the transition would be to enforce on single crystals, over a range of temperature, a deformation difficult to accommodate by known mechanisms: in particular, c-axis compression. As a refinement, it was further decided to restrict the expansion to only one direction, or to enforce the state of plane strain which is also of much practical interest in a variety of deformation processing operations. In that way, if expansion were confined to $\langle 11\bar{2}0 \rangle$, it might be expected that shape change would be accommodated best by slip or twinning on planes of the form $\{11\bar{2}x\}$ (Fig. 2a).

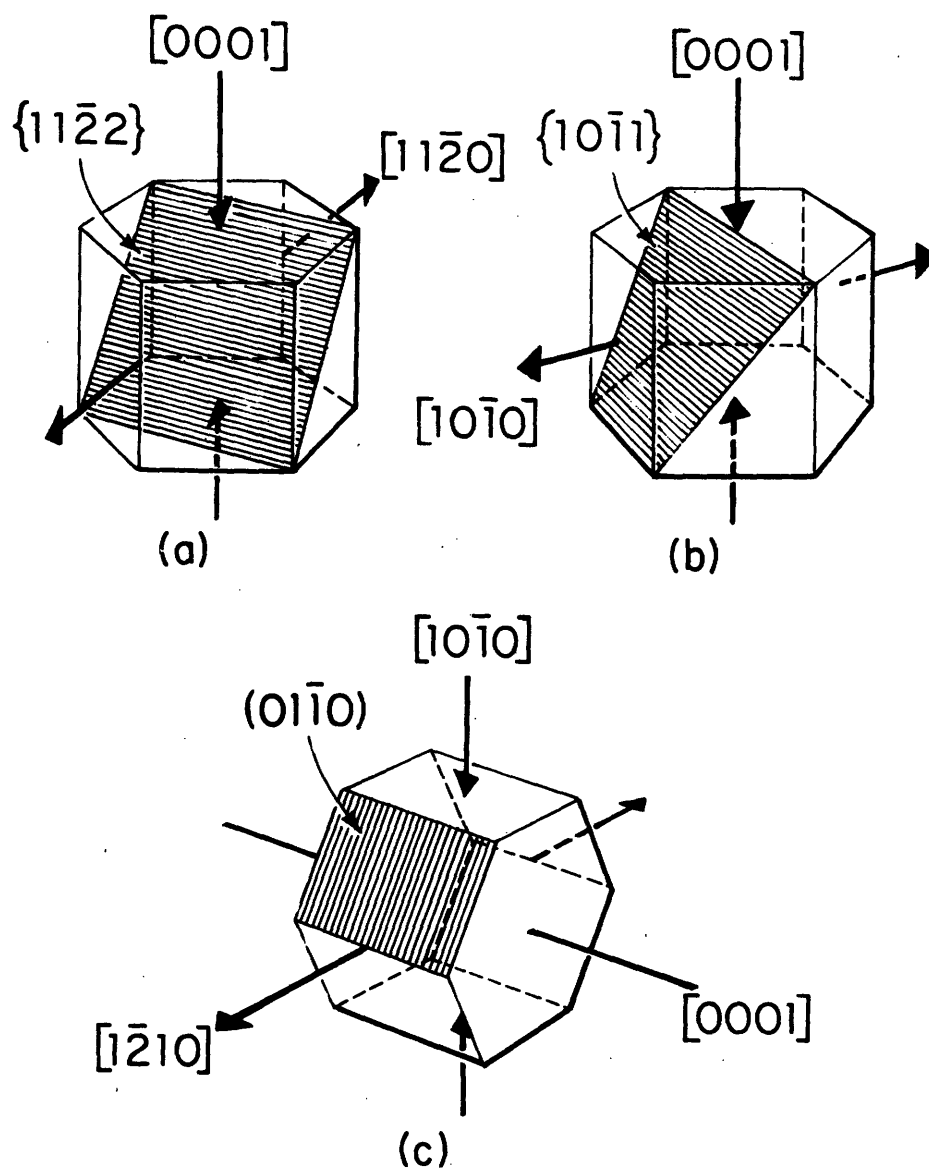


Fig. 2. Proposed Compression Experiments

(a) Parallel to the $[0001]$ c-axis with expansion limited to $[11\bar{2}0]$; it might be expected that slip or twinning on planes of the form $\{11\bar{2}x\}$ would be favored.

(b) Parallel to $[0001]$ with expansion limited to $[10\bar{1}0]$; now slip or twinning on planes of the form $\{10\bar{1}x\}$ might be favored.

(c) Normal to $[0001]$ but without expansion along that axis; pyramidal or prismatic $\{10\bar{1}0\}$ slip ought to be encouraged since the basal plane is unstressed and $\{10\bar{1}2\}$ twinning must lead to an expansion in the direction of restraint.

If the expansion were limited to the $\langle 10\bar{1}0 \rangle$, shear on planes of the form $\{10\bar{1}x\}$ ought to be encouraged (Fig. 2b). As a final variation, experiments were planned for compression normal to the c-axis but without expansion along that axis (Fig. 2c). Now the encouragement should go to pyramidal and prism-plane slip since the basal plane would be unstressed and $\{10\bar{1}2\}$ twinning would produce expansion in the direction of restraint. How sound those speculations proved to be is brought out in what follows.

EXPERIMENTAL PROCEDURES

Specimen Preparation: Single crystals measuring $1/8 \times 1/4 \times 5$ in. were grown by the Bridgman technique from sublimed magnesium containing less than 0.04% total impurities. A "soft" mold of tightly packed graphite powder was used in an atmosphere of anhydrous sulphur dioxide. Details are given in Appendix 1. The orientation of each crystal was determined from a Laue back-reflection photograph, and was within 1.5° of the orientation quoted in the text. The crystals were lightly etched in 25% hydrochloric acid and cut with an acid saw into small test pieces about $5/8$ in. long. Although the initial blanks were machined parallel within ± 0.0001 in., 1-mil asperities produced during crystal growth were present on the final test pieces.

Testing: To achieve plane-strain compression, the crystal was held in an adjustable vise-like channel. The walls restricted lateral

spreading while permitting flow down the axis of the channel (Fig. 3). The sample was compressed with an indenter of width approximately equal to twice the crystal thickness. The bottom of the channel was well lubricated (as noted below); if it is imagined to have been frictionless, the configuration was equivalent to the simpler case of compression between two indentors of width equal to sheet thickness, which represents reasonably homogeneous straining with little contribution from friction to the applied stress.

The sample, channel, and indenter were degreased with trichloroethylene and lubricated with a colloidal molybdenum disulphide spray (Aerolon M). To assure an initially tight fit, without straining the crystal, the vise was brought up finger-tight on an indenter which was larger than the width of the crystal by no more than 0.0005 in. The assembly was then placed in a compression fixture with platens parallel to within 0.01°. Tests were made at a speed of 0.02 in./min. in an Instron machine. Displacement was measured with a differential transformer and plotted simultaneously with the load on the Instron X-Y recorder. High temperature tests were conducted under heated silicone oil (Dow Corning 710) and the temperature of the sample was controlled to within $\pm 2^\circ\text{C}$ of the reported value.

Identical procedures were followed for plane-strain tests on the polycrystalline magnesium (of mean grain diameter about 4×10^{-4} in.) from which the single crystals were grown. Under metallographic examination with polarized light, the material was found to be textured, somewhat diffusely but with [0001] poles clustered around the sheet normal and spreading outwards by as much as 50° .

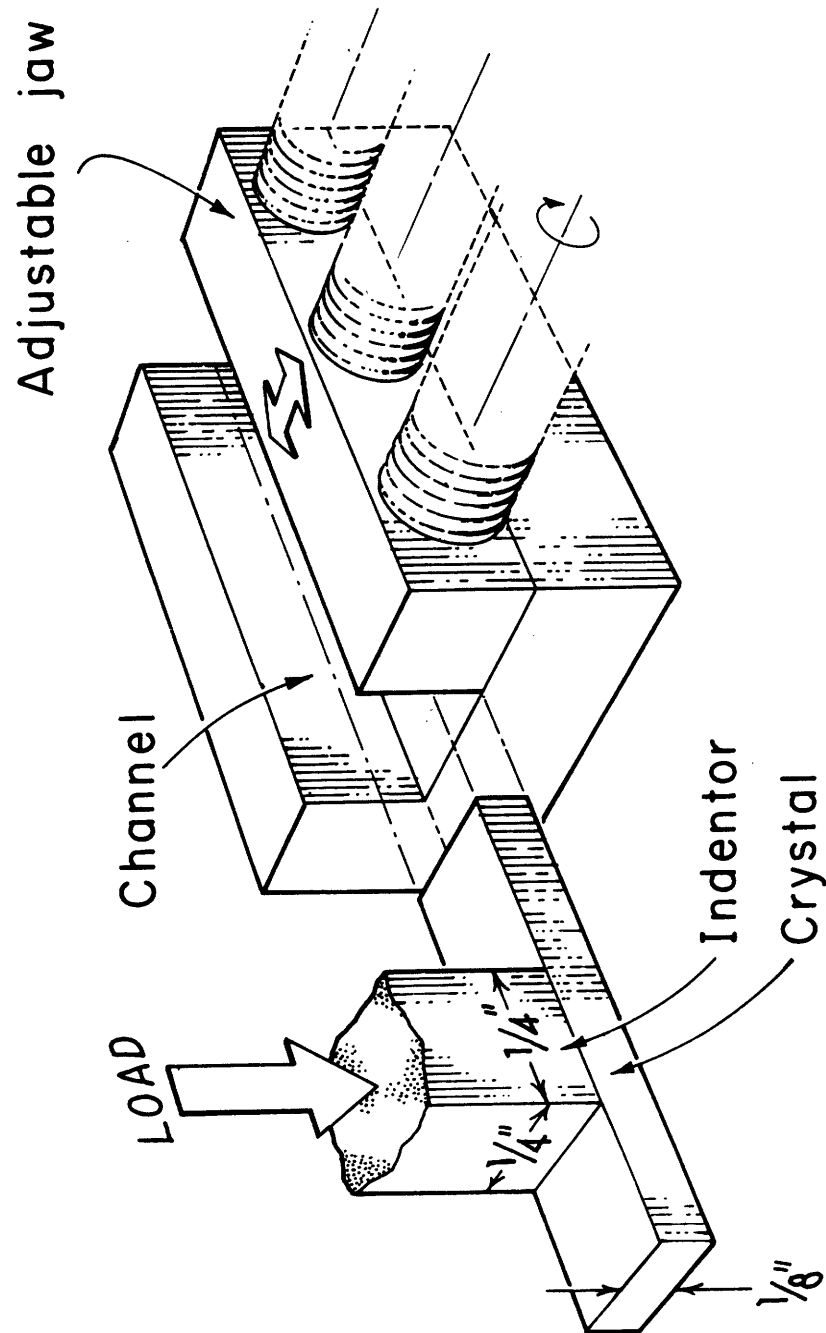


Fig. 3. Schematic Arrangement of Crystal, Indenter and Channel for Enforcing Plane Strain. The adjustable jaw restricts lateral spreading during compression and is supported by 3- $\frac{1}{4}$ x 20 hardened cap screws.

Analysis of Data: True-stress: true-strain curves were calculated from the load-displacement data. Using typical values for the friction coefficient of molybdenum disulphide of 0.06 to 0.12, a conservative estimate of the contribution of friction to the applied stress does not exceed 6 to 12%.^{10,11}

An initial region of upward curvature was present in all stress-strain curves, although it was not reproducible. Its extent was 1 to 3% strain, which was consistent with the strain for flattening the asperities on the growth surfaces. Intentional surface roughening acted to lengthen the region (Appendix 1). Also, translation along the strain axis brought curves of identical specimens with varying surface roughness into coincidence, except for the initial low-stress curvature. Therefore, that particular detail was eliminated by the somewhat arbitrary method of displacing all stress-strain curves until the characteristic linear region, following the curvature, passed through the origin.

Metallographic Examination: After testing, all samples were mounted in a cold setting resin, ground on 800 silicon carbide paper, and electropolished using Jacquet's method.¹² Each was then etched in acetic picral after Pearsall¹³ and examined under polarized light to observe the trace of the basal plane on the viewing surface. All habit planes of twins were determined by two-surface analysis.¹⁴ In general, sectioning was done in the plane of flow (defined by the loading direction and direction of extension) or in the transverse (orthogonal) plane.

RESULTS

Compression Parallel to the c-axis

The true-stress:true-strain curves with expansion limited to either $\langle 1\bar{2}10 \rangle$ or $\langle 10\bar{T}0 \rangle$ are presented in Figs. 4 and 5, respectively. Although plotted separately, the curves are too much alike for separate consideration. Nor were the metallographic observations basically sensitive to the difference in constraint direction. Therefore, little was gained by this first refinement in testing procedure.

Room Temperature: Initial work hardening was rapid and followed by fracture after about 6% strain at a stress of 47 to 53 ksi. Behavior along the linear portion of the stress-strain curve was not fully elastic since basal slip lines were visible on unconstrained crystals which hardened along a similar path, and a plastic set on unloading could be measured with a micrometer. Beyond that, the slope at room temperature was only about $E/5$ (E = Young's modulus), while the temperature dependence of the slope was an order of magnitude greater than that of the modulus.⁸

Nothing but basal slip can be inferred from the initial hardening rate. In the first place, slip on (0001) can be caused by misalignment of as little as 0.15° , owing to the low critical resolved shear stress (~ 70 psi).⁸ Also, $d\sigma/d\epsilon = (1/m^2)(d\tau/d\gamma)$, where m is the Schmid orientation factor and $d\tau/d\gamma$ is the basal shear-hardening rate. If

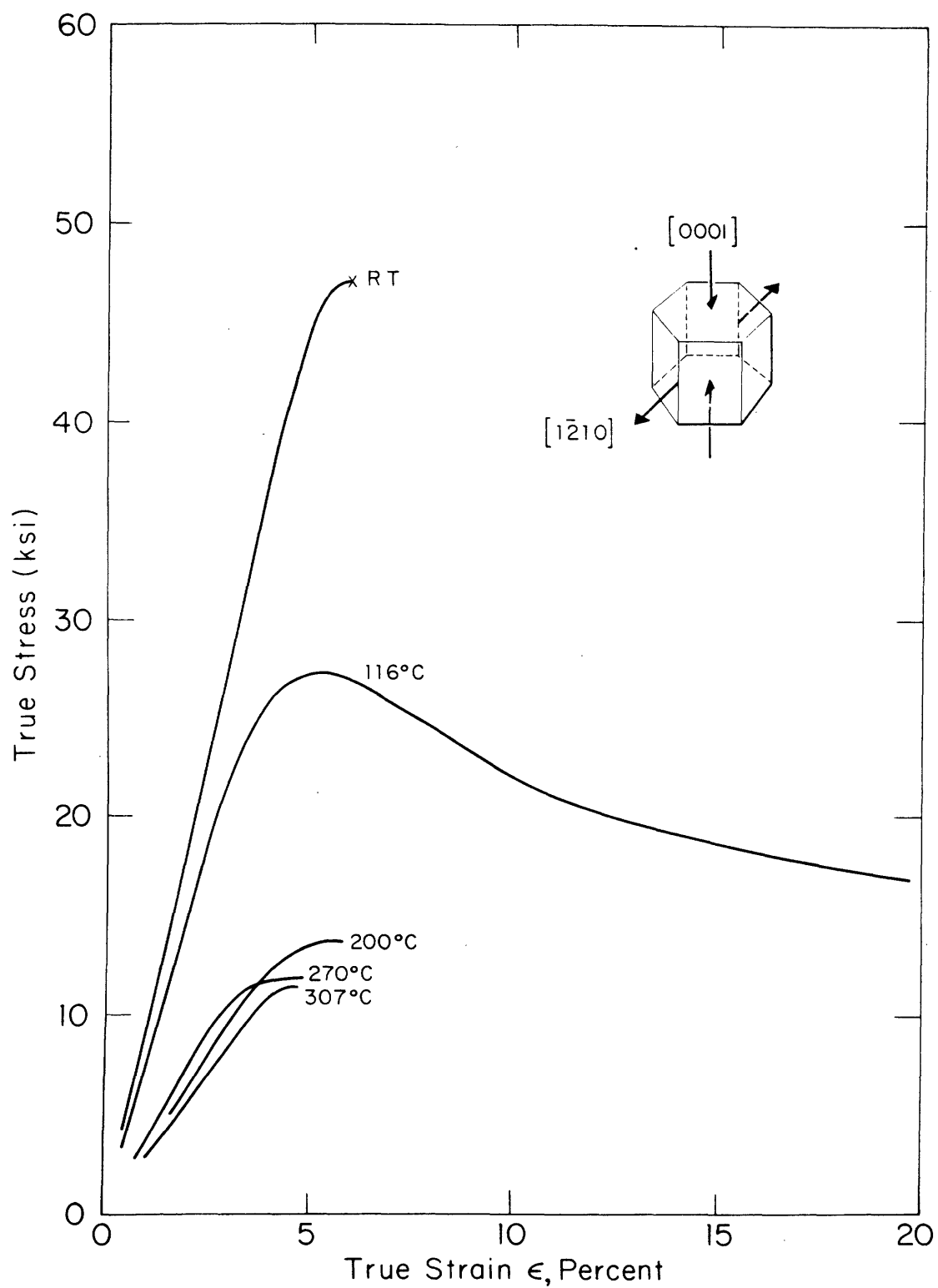


Fig. 4. True-stress: true-strain Curves for Magnesium Crystals Compressed Along the $[0001]$ c-axis with Expansion Limited to $[1\bar{2}10]$.

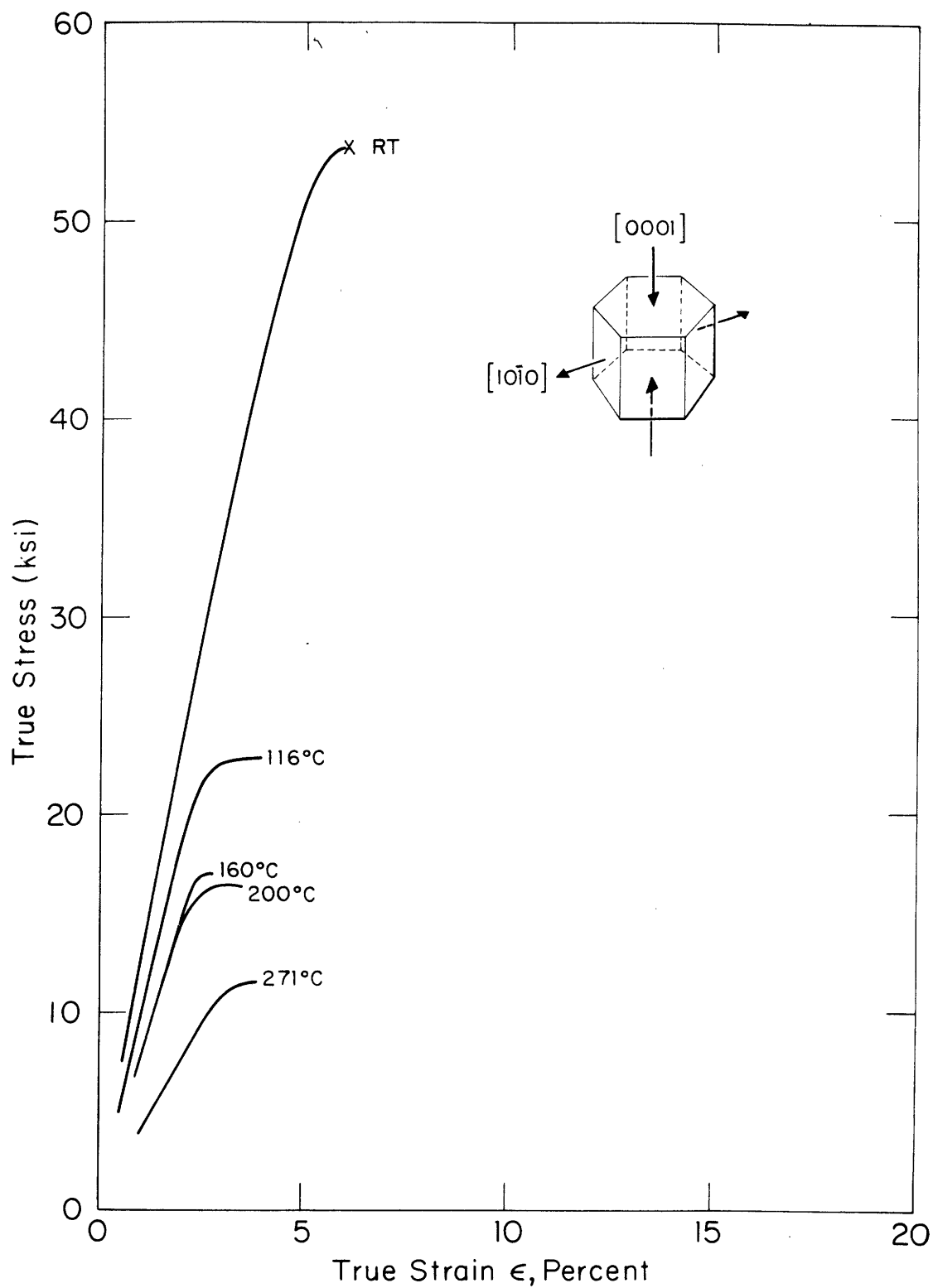


Fig. 5. True-stress: true-strain Curves for Magnesium Crystals Compressed Along the [0001] c-axis with Expansion Limited to [1010]

m were as large as 2.6×10^{-2} (allowing a misorientation of 1.5°) and $d\tau/d\gamma \approx 10^{-4} \mu$ at room temperature¹⁵ (μ = shear modulus), $d\sigma/d\epsilon \approx 0.1 \mu$ which is nearly what was observed. In addition, the temperature dependence of the shear hardening rate is essentially that observed here.¹⁵

Twinning on $\{10\bar{1}1\}$ primarily, and on $\{10\bar{1}3\}$ to a much smaller extent, was associated with the final, sharply curved portion of the stress-strain curves. From metallographic examination within a half-hour after fracture, it was clear that recrystallization had begun in the $\{10\bar{1}1\}$ bands (Fig. 6). Also, the basal plane was within 10° of the plane of the band, which is to be expected from slip following the double twinning sequence; that represented a rotation, induced by slip, of 22.5° from the orientation left by twinning (Fig. 1c).

The twins were not evenly distributed, but appeared in a narrow zone, beginning at the indenter edge, in which shear fracture eventually occurred (Fig. 7). The curves bent over so abruptly that the maximum stress, σ_{\max} , could be used in calculating a "critical" shear stress for twinning on $\{10\bar{1}1\}$ along $\langle 10\bar{1}2 \rangle$. Results from several tests are listed in Table I. No twins of the form $\{11\bar{2}x\}$ were observed, even in crystals forced to expand along $\langle 11\bar{2}0 \rangle$.

The fracture surface was cleavage-like in appearance, but its orientation (30° - 40° from the basal plane) was variable and did not correspond to any plane of low indices. In an initially polished crystal compressed

TABLE I
Resolved Shear Stresses for {1011}
Twinning at Room Temperature

Direction of Compression	Direction of Expansion	σ_{\max} (ksi)	τ for {10 $\bar{1}$ 1} <10 $\bar{1}$ 2> Twinning (ksi)
[0001] (c-axis)	[10 $\bar{1}$ 0]	53.4	22.3
[0001] (c-axis)	[11 $\bar{2}$ 0]	47.0	19.6
[10 $\bar{1}$ 0]	[1 $\bar{2}$ 10]	39.1	12.2
[1 $\bar{2}$ 10]	[10 $\bar{1}$ 0]	35.3	11.0

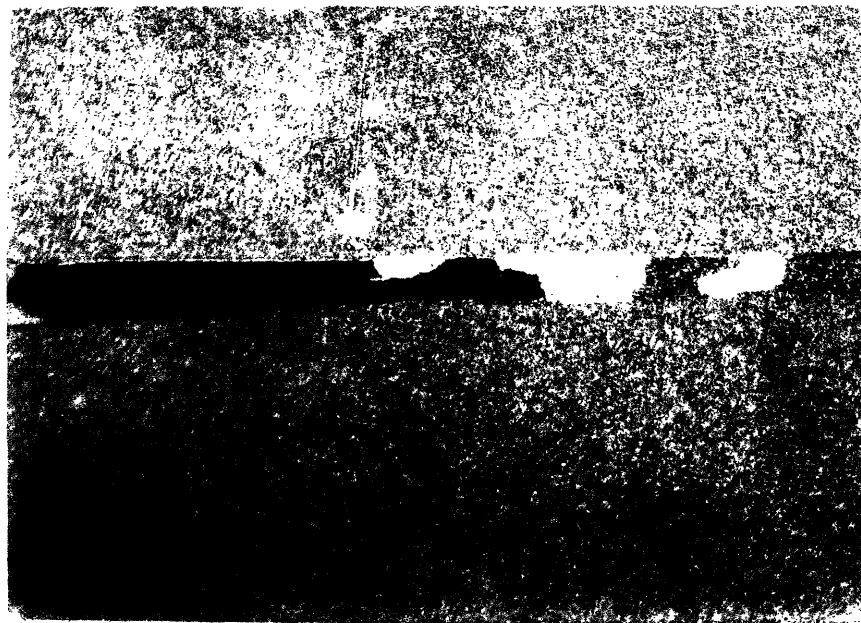


Fig. 6. Recrystallization in a Doubly Twinned Band Along $\{10\bar{1}1\}$ Formed at Room Temperature. This observation made about a month after deformation, although recrystallization was apparent in examination within one-half hour. 500X under polarized light. Plane of view (0001). Etched in acetic picral.

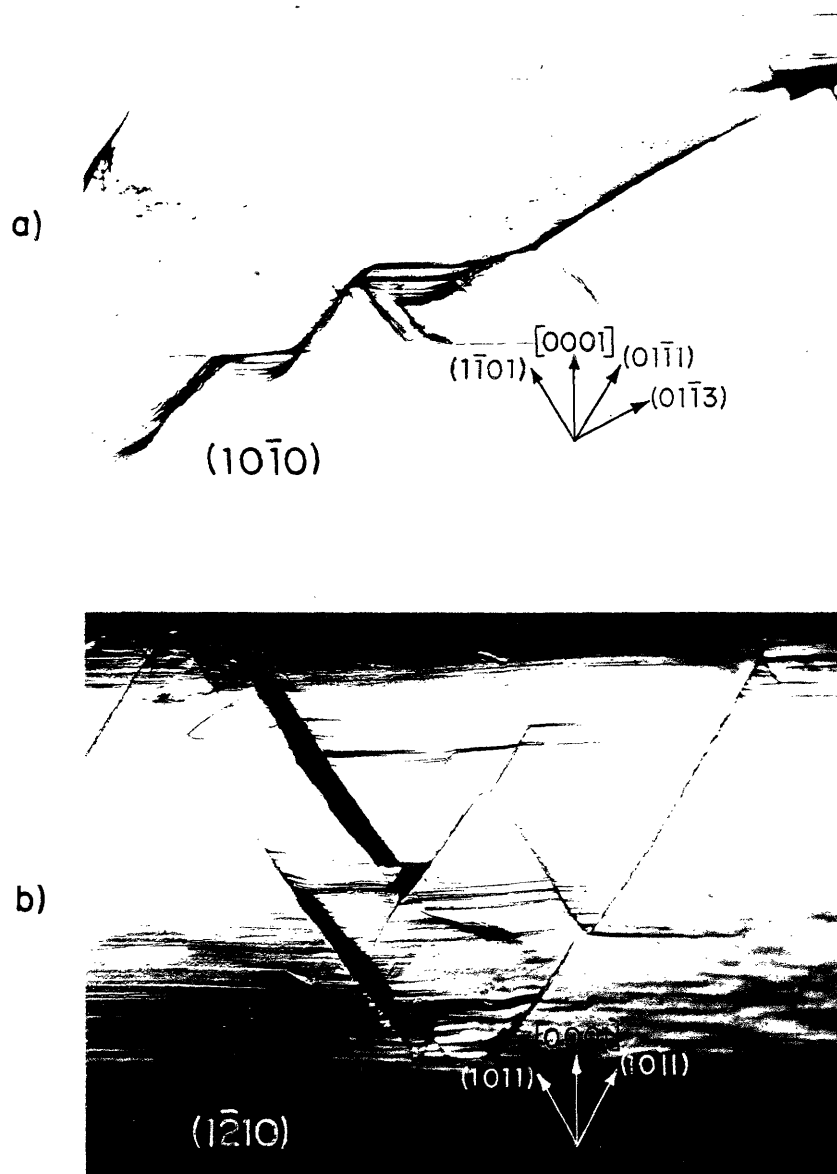


Fig. 7. Fracture Near the Indenter Edge in c-axis Compression at Room Temperature.

- (a) Cracking along $\{10\bar{1}1\}$ and $\{10\bar{1}3\}$ at a prepolished surface. Unetched 100X.
- (b) Cracking along $\{10\bar{1}1\}$ exclusively; surface curved in prepolishing. Unetched 100X.

without constraint, fracture involved the linking of cracks in $\{10\bar{1}1\}$ and $\{10\bar{1}3\}$ twin bands (Fig. 7).

Because of loading through an indenter, the deformation zone was enclosed by elastic-plastic boundaries. To discover any effect of such boundaries, they were removed from two crystals by applying load with a platen that extended beyond the edges of the crystals; both fractured after 6% strain at a stress within 10% of that observed in the indented crystals.

Although $\{10\bar{1}2\}$ twinning causes expansion along the c-axis, many $\{10\bar{1}2\}$ twins were (unexpectedly) found throughout all crystals compressed in that direction (Fig. 8a). To determine their origin, another chemically polished crystal was squeezed along the c-axis in a vise while being observed at 100X. Only basal slip lines were visible on loading, but as the load was released many large $\{10\bar{1}2\}$ twins appeared, presumably because of residual stresses due to non-homogeneous flow. Since the normal stress for $\{10\bar{1}2\}$ twinning is only about 0.6 ksi, a residual stress less than 2% of that applied would have produced these twins.

Elevated Temperature: As the temperature was increased towards 300°C, σ_{\max} dropped about 75% (Fig. 9). None of the crystals were deformed to fracture; as the load maximum was passed, straining continued under falling stress. That behavior is indicated in Fig. 4 for the crystal at 116°C, which finally acquired a few cracks after about 40% reduction. Other tests were halted shortly after the

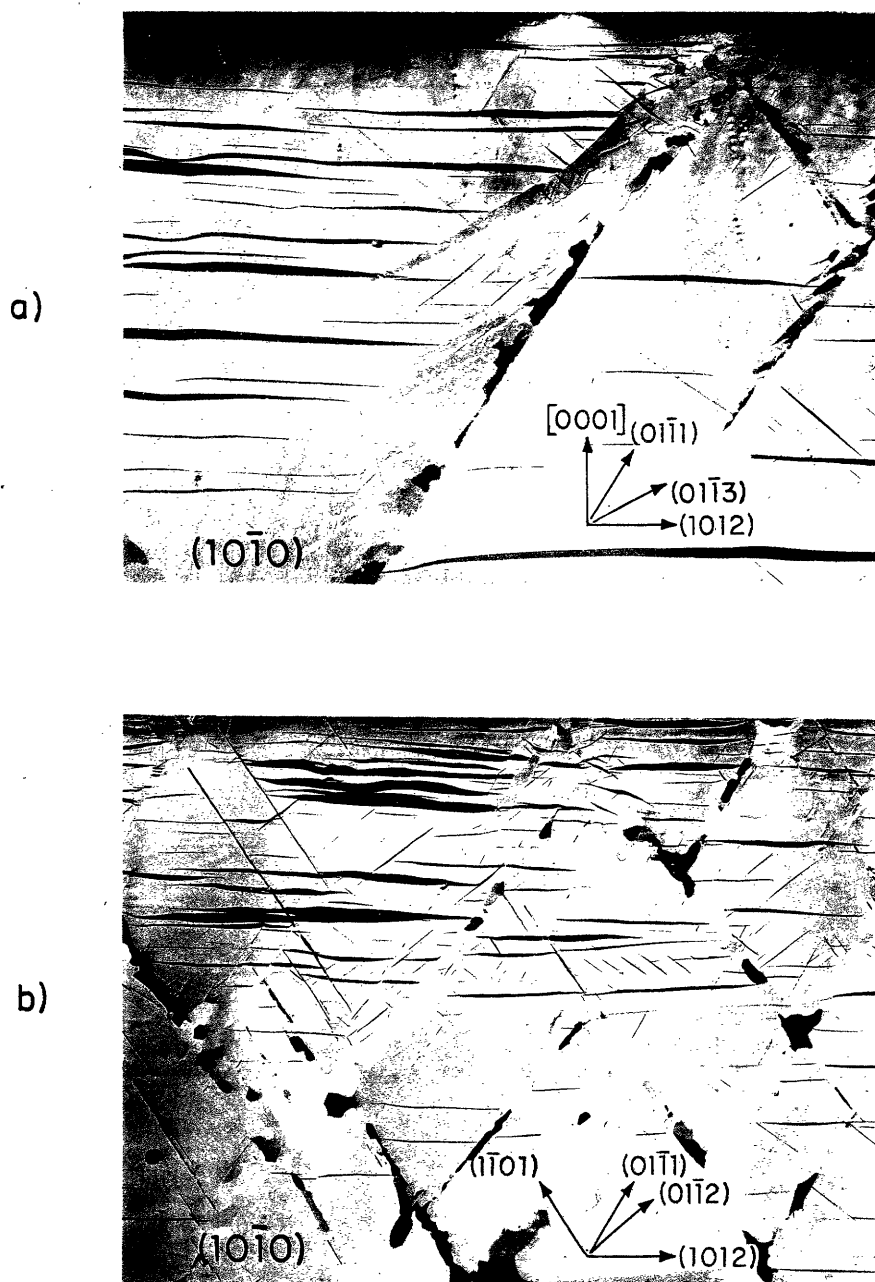


Fig. 8. Twinning at Elevated Temperatures in Magnesium Crystals Compressed Along $[0001]$. 40X, under polarized light. Etched in acetic picral.

- (a) 200°C ; $\{10\bar{1}1\}$ bands are recrystallized, $\{10\bar{1}3\}$ are not. Dark, horizontal $\{10\bar{1}2\}$ twins formed on unloading.
- (c) 272°C ; $\{10\bar{1}1\}$ recrystallized bands.

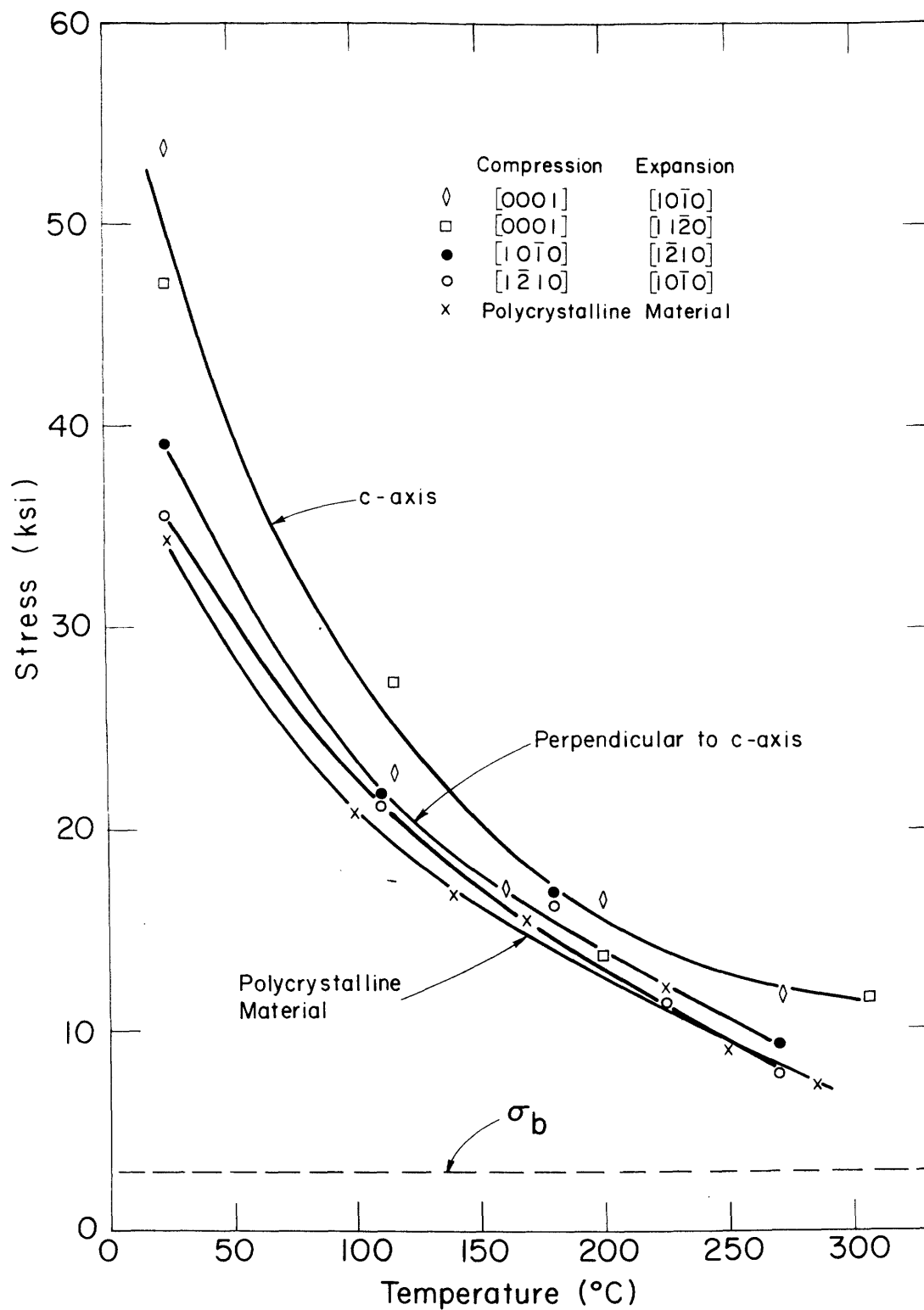


Fig. 9. Maximum stress σ_{\max} versus temperature. Dashed line σ_b indicates an estimate of normal stress for basal slip within a $\{10\bar{1}1\}$ twin in c-axis compression. Full lines represent experimental data for compression along stated directions.

maxima so that metallographic examination might be made on only lightly deformed structures.

Much more twinning was evident now (Fig. 8). Yet only the more numerous $\{10\bar{1}1\}$ bands were consistently recrystallized, which suggests again that most of the shear occurred within them. As at room temperature, the basal plane in the twinned (and recrystallized) material was rotated about 20° towards the plane of the band. In $\{10\bar{1}3\}$ bands, however, the basal plane lay within $\pm 5^\circ$ (\sim experimental uncertainty) of the double twinning orientation (Fig. 1e). There were no $\{10\bar{1}3\}$ bands at 270°C or above.

With heavier deformation (40% at 116°C) the twin band was also rotated, in this example from a predicted 62° (Fig. 1b) to an observed 30° (Fig. 10). A similar rotation of shear bands was found in cold-rolled alloys by Couling, Pashak, and Sturkey.⁶

Polycrystalline Material

The true-stress:true-strain curves are given in Fig. 11, and the σ_{max} values are included in Fig. 9. Cracking was not evident after increasing temperature from 170°C to 224°C ; the transition must lie at about 200°C .

Compression Perpendicular to the c-axis

The true-stress:true-strain curves for the various temperatures are presented in Figs. 12 and 13, where differences are now significant.

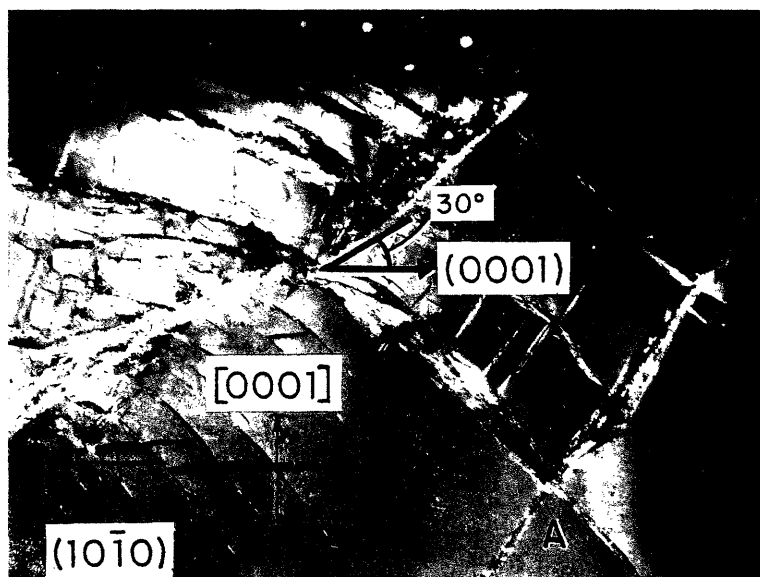


Fig. 10. Rotation of $\{10\bar{T}1\}$ Bands During 40% Compression Along $[0001]$ at 116°C . Initially, bands at A were near the indenter edge, but were moved out from under the indenter during the test; thus they underwent less than the full deformation and so are still located along $\{10\bar{T}1\}$. With heavier deformation towards the center, bands were rotated away from the loading axis, to make a final angle of about 30° with the basal plane. 40X under polarized light. Etched in acetic picral.

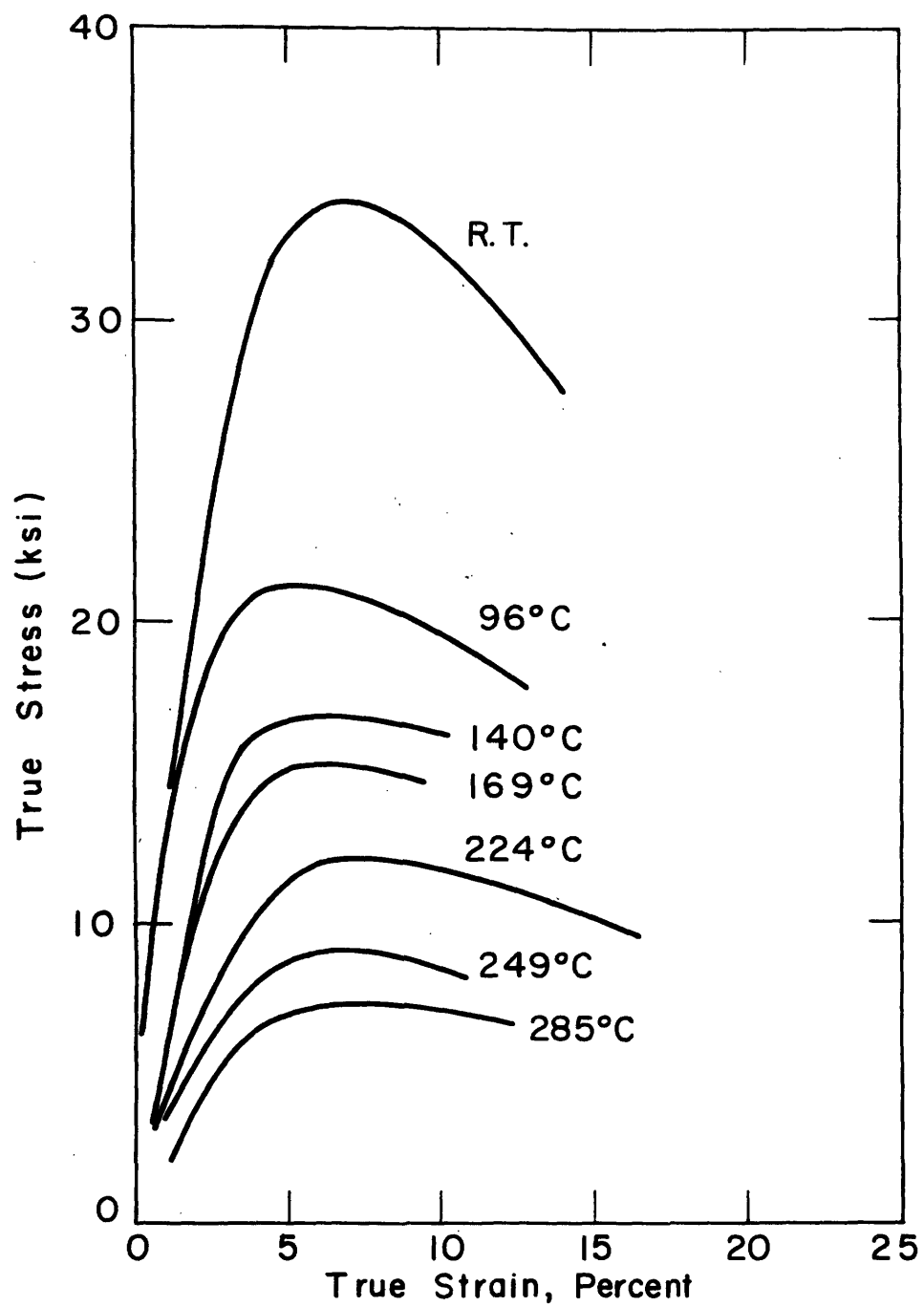


Fig. 11. True-stress: true-strain Curves for Plane-strain Compression of Polycrystalline Magnesium.

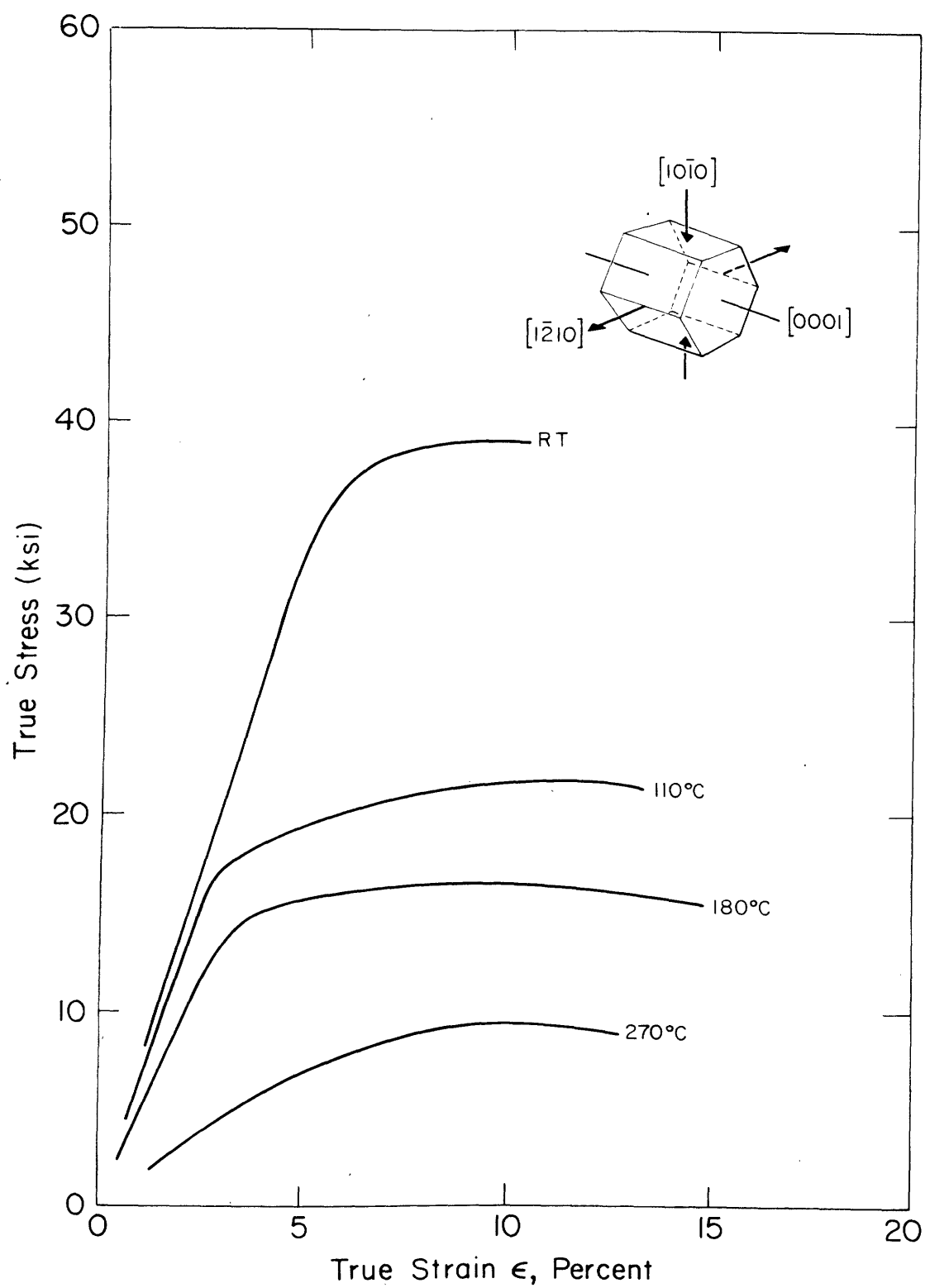


Fig. 12. True-stress: true-strain Curves for Magnesium Crystals Compressed Along $[10\bar{1}0]$ with Expansion Limited to $[1\bar{2}10]$.

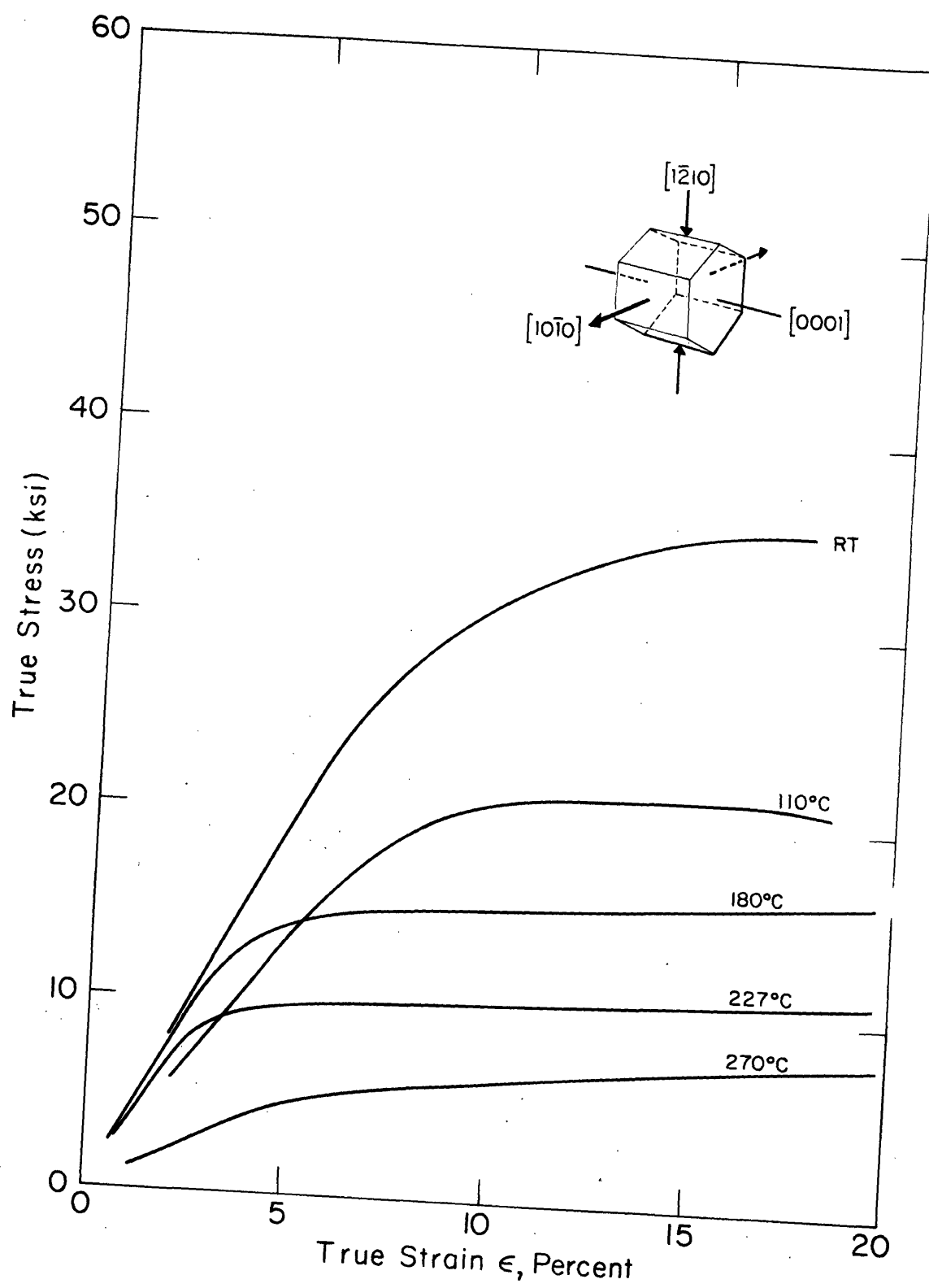


Fig. 13. True-stress: true-strain Curves for Magnesium Crystals Compressed Along $[1\bar{2}10]$ with Expansion Limited to $[10\bar{1}0]$.

Room Temperature: Perhaps the most obvious way of accommodating compression normal to the c-axis without producing strain along that axis is by some form of nonbasal slip (Fig. 2c); nevertheless, the deformation was found, by means of interrupted testing, to involve twinning. In both series of tests, $\{10\bar{1}2\}$ twins, which lead to c-axis expansion, appeared during the initial linear region of the stress-strain curves. At the lower temperatures, the corresponding hardening rates were most different (Table II). Both, however, were roughly E/10 and higher by about an order of magnitude than that for compression (along $[10\bar{1}0]$) of an unconstrained crystal. Thus much of the initial hardening was associated with the reaction stresses at the channel wall.

A numerical estimate of the hardening from that source, based on the assumption that plastic strain along the c-axis (from twinning) is accommodated by elastic deformation in the channel, leads to (Appendix 2)

$$\theta \approx K \left(\frac{m_r}{m_a} \right)^2 \quad (1)$$

where K is the transverse stiffness of the channel, and m_r and m_a are, respectively, Schmid factors for $\{10\bar{1}2\}$ twinning relative to applied (a) and reaction-stress (r) directions. With the appropriate Schmid factors (Table II), $\theta_{[10\bar{1}0]}/\theta_{[1\bar{2}10]} = 1.78$, which is about what is reported in Table II.

TABLE II
Initial Linear Hardening Rate for Compression Perpendicular to the c-axis

Compression Axis	Hardening Rate	Temperature					Schmid Factors for {10 $\bar{1}$ 2} Twinning	
		RT	110°C	180°C	227°C	270°C	m_r	m_a
[10 $\bar{1}$ 0]	$\theta = \frac{d\sigma}{d\epsilon} (10^6 \text{ psi})$	0.865	0.730	0.521	---	0.151	-0.499	0.499
	$\theta/E (\%)$	15.0	13.6	10.4	---	3.3		
[1 $\bar{2}$ 10]	$\theta = \frac{d\sigma}{d\epsilon} (10^6 \text{ psi})$	0.447	0.283	0.407	0.347	0.207	-0.499	0.375
	$\theta/E (\%)$	7.7	5.3	8.1	7.3	4.5		

Straining along the more nearly horizontal sections of both sets of curves was associated with twinning on $\{10\bar{1}1\}$ in previously untwinned material. That could only have happened to relieve the c-axis expansion which had been generated by $\{10\bar{1}2\}$ twinning (Fig. 14). The maximum stresses (some of which do not appear on the stress-strain curves) are included in Fig. 9.

Such cooperative twinning reflects the difficulty of $\{10\bar{1}0\}$ and $\{10\bar{1}1\}$ slip along $\langle 11\bar{2}0 \rangle$. The specimens were not useful for slip-trace studies especially of nonbasal traces which have proved so difficult to observe.^{16,17} Yet there is evidence of $\{10\bar{1}0\}$ or $\{10\bar{1}1\}$ slip in the experimental temperature range,¹⁶⁻²⁰ and especially of $\{10\bar{1}0\}$ above about 180°C.²⁰ Using σ_{\max} values, resolved shear stresses on these systems at room temperature were calculated to be 15 to 17 ksi for $\{10\bar{1}0\}$ slip and 13 to 15 ksi for $\{10\bar{1}1\}$ slip. From data of Flynn, Mote and Dorn,²⁰ the critical resolved shear stress on $\{10\bar{1}0\} \langle 11\bar{2}0 \rangle$ for a mixture of prismatic slip and $\{10\bar{1}2\}$ twinning at the beginning of plastic deformation is about 7 ksi. The strain rate sensitivity of nonbasal slip has been determined by Reed-Hill and Robertson¹⁶ in tests similar to those of Flynn *et al.*²⁰ Adjusting the formers' data for the strain rate in the present work, the expected shear stress would be roughly 14 ksi for the prismatic case. The agreement seems too close to be fortuitous, and it is probably in order to associate some nonbasal slip with $\{10\bar{1}1\}$ twinning.

A stress for $\{10\bar{1}1\}$ twinning can also be calculated by assuming that the applied and reactive stresses must satisfy the shear-stress requirements

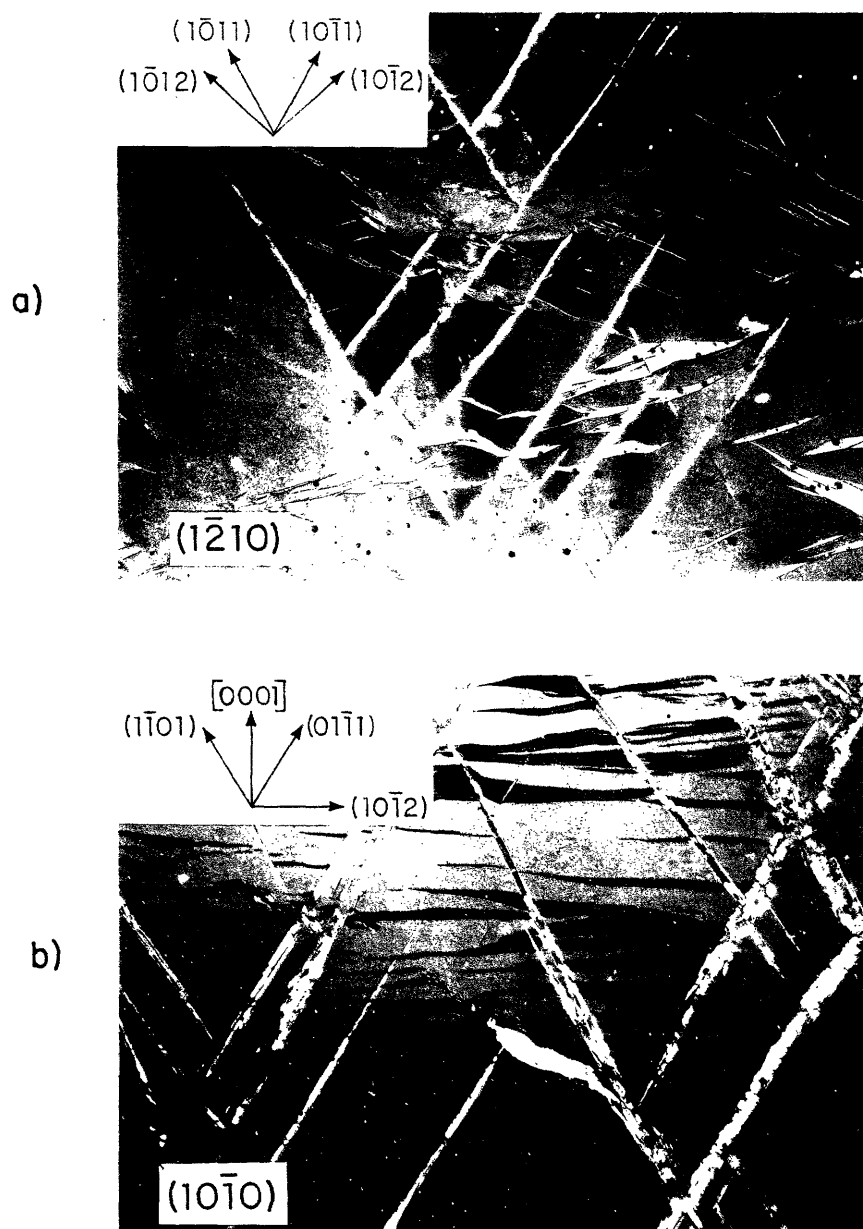


Fig. 14. $\{10\bar{1}2\}$ Twins and $\{10\bar{1}1\}$ Doubly Twinned Volumes in Magnesium Crystals After Compression Perpendicular to $[0001]$. 40X under polarized light. Etched in acetic picral.

- (a) Compression along $[1\bar{2}10]$. Two different sets of $\{10\bar{1}2\}$ twins were formed. Most of the $\{10\bar{1}1\}$ appeared to penetrate $\{10\bar{1}2\}$ twins.
- (b) Compression along $[10\bar{1}0]$. Only a single set of $\{10\bar{1}2\}$ twins appeared and was penetrated by $\{10\bar{1}1\}$.

for twinning on both $\{10\bar{1}2\}$ and $\{10\bar{1}1\}$ simultaneously. The key equations for $[10\bar{1}0]$ compression and restraint along the c-axis are:

$$\tau(0\bar{1}11)[0\bar{1}1\bar{2}] = -0.104 \sigma_a + 0.416 \sigma_r$$

$$\tau(10\bar{1}2)[10\bar{1}1] = 0.499 \sigma_a - 0.499 \sigma_r$$

where σ_a and σ_r are the applied and transverse reaction stresses, respectively, (the former being σ_{\max} from Fig. 9) and the numerical coefficients are the Schmid factors appropriate for the biaxial loading, those for $(10\bar{1}2)[10\bar{1}1]$ twinning having been given in Table II. Further detail is found in Appendix 3. Experimentally, $\tau(10\bar{1}2)[10\bar{1}1] \ll \sigma_a$. Therefore, $\tau(0\bar{1}11)[0\bar{1}1\bar{2}] \approx 0.312 \sigma_a$. The same solution happens to apply for compression along $[1\bar{2}10]$. Numerical results are also listed in Table I ($\sigma_a = \sigma_{\max}$), where it appears that a change in loading direction from $[0001]$ to $[10\bar{1}0]$ is accompanied by a 40% drop in the calculated resolved shear stress for twinning on $\{10\bar{1}1\}$. With a further change in direction from $[10\bar{1}0]$ (Fig. 12) to $[1\bar{2}10]$ (Fig. 13) the stress is lowered an additional 10%. Thus there is no critical resolved shear stress for $\{10\bar{1}1\}$ twinning which can be found by a simple application of Schmid's law.

In both directions of compression, the crystals were much more ductile than those squeezed parallel to $[0001]$. No cracks were observed after 18% reduction along $[1\bar{2}10]$. Along $[10\bar{1}0]$, however,

after 12-14% reduction at room temperature, a few cracks about 10 mils in length were found in $\{10\bar{1}1\}$ twin bands near the indenter edge; raising the deformation temperature to 110°C acted to shorten the cracks to about 1 mil, while none appeared above 180°C .

Most of the $\{10\bar{1}1\}$ twins penetrated the $\{10\bar{1}2\}$ as if the latter were no barrier (Fig. 14). Perhaps the reason is that (choosing a specific case) a twin on $(01\bar{1}1)$ could be continued through another on $(10\bar{1}2)$ by the formation within the $(10\bar{1}2)$ twin of a $(0\bar{1}11)$ twin rotated only slightly ($< 1^{\circ}$) from the original $(01\bar{1}1)$. Details are given in Appendix 4. Some $10\bar{1}1$ twins, however, are stopped, apparently because not all inter-sections allow that relationship to be satisfied.

Elevated Temperature: At 270°C there were no $\{10\bar{1}1\}$ and too little $\{10\bar{1}2\}$ twinning (no more than 20 volume percent) to accommodate the 15-20% imposed strain; thus, there was even more reason for concluding that something else happened. The critical resolved shear stress calculations can be made as a function of temperature; being based on σ_{max} they have the same temperature dependence. At 270°C , the critical resolved shear stress for initiating prismatic slip is about 0.87 ksi.²⁰ Adjusting for strain rate as before, that value becomes 1.74 ksi which corresponds reasonably well with values of 1.73 to 2.21 ksi at the upper end of the initial linear regions of both curves in Figs. 12 and 13.

DISCUSSION

{10 $\bar{1}$ 1} Twinning: One way of rationalizing the absence of a critical resolved shear-stress law for {10 $\bar{1}$ 1} twinning has already been given by Bell and Cohn²¹ and by Price.²² In zinc and cadmium, {10 $\bar{1}$ 2} twinning had to be preceded by stress concentration at the twin site. This was derived from the intersection of slip on basal planes and a system with a nonbasal slip vector in zinc;²¹ in dislocation-free cadmium foils, twins always occurred at notches along the edges of the foils.²²

A certain pattern of stress concentration from prior shear is indicated in the present work. In compression perpendicular to the c-axis the eventual reduced hardening rate is accompanied by metallographically obvious twinning on {10 $\bar{1}$ 1} and, by inference from flow stress measurements, some nonbasal slip. Perhaps intersections among different systems in {10 $\bar{1}$ 0} <11 $\bar{2}$ 0> and/or {10 $\bar{1}$ 1} <11 $\bar{2}$ 0> provide the necessary stress concentrations for the twinning. The temperature dependence of that kind of slip might then underlie the temperature dependence of σ_{\max} along the appropriate curves in Fig. 9. In such a vein, the polycrystalline material could be expected to offer the most opportunity for internal stress concentration, and it supports (by a very small amount) the lowest σ_{\max} .

No evidence has been found in this work of a slip vector out of the basal plane. As noted, however, the experiments were not suited

for detecting small amounts of such slip, which has been encountered in zinc,²¹ cadmium,²² and beryllium.²³ Therefore, some might occur. If it did, it would also be more thermally activated than basal slip. If, in addition, the intersection of that slip with basal slip was the prerequisite for $\{10\bar{1}1\}$ twinning in c-axis compression, this would be a basis for understanding the higher but similarly temperature dependent σ_{\max} in Fig. 9.

Plasticity Transition: The transition is governed by more than the stress for $\{10\bar{1}1\}$ twinning, although operation of the double twinning mechanism without fracture must be essential for ductility in polycrystalline material as well as in single crystals reduced along the c-axis.

Whether there is fracture or not ought to be influenced by the difference, $\Delta\sigma$, between the stress for $\{10\bar{1}1\}$ twinning, σ_{\max} (Fig. 9), and the stress for flow (basal slip) within the twinned volume, σ_b , acting in the same direction as σ_{\max} . In general,

$$\sigma_b = K [\tau_{(0001)}/m] \quad (2)$$

where $\tau_{(0001)}$ is the shear stress for basal slip and K is a factor of perhaps 20, representing the increased difficulty of basal slip within a twin.²¹ However, the temperature dependence of σ_b should be that $\tau_{(0001)}$, and therefore low.¹⁵ In c-axis compression, after double twinning, $\sigma_b = 3$ ksi and that has been included in Fig. 9. In

compression along $[1\bar{2}10]$, $m \approx 0$ both before and after the twinning under side-wall pressure, and $\sigma_b \rightarrow \infty$ unless nonbasal slip is considered; then σ_b becomes finite but still large. In compression along $[10\bar{1}0]$, $m \approx 0.37$ in the $\{10\bar{1}1\}$ twin and $\sigma_b \approx 4$ ksi.

Considering only basal slip, $\Delta\sigma$ decreases rapidly with increasing temperature. One possible consequence is that shear strain in the twin from basal slip will also drop. To demonstrate, it can be assumed that all elastic strain energy, U_e , released in unloading (locally) from σ_{\max} to σ_b is dissipated by slip within the twinned volume as U_p . Now,

$$U_e = \frac{V_s}{2E} (\sigma_{\max}^2 - \sigma_b^2)$$

$$U_p = V_t \int \tau_b d\gamma_b \approx V_t \left(\frac{\sigma_b}{2} \gamma_b \right)$$

where V_s is the volume of stressed material, V_t is the twinned volume, E is the elastic modulus, and γ_b is the shear strain. Equating U_e and U_p , and taking $\sigma_b^2 \ll \sigma_{\max}^2$,

$$\gamma_b \approx \frac{\sigma_{\max}^2}{\sigma_b E (V_t/V_s)} \quad (3)$$

The more extreme example is c-axis compression. Metallographic estimates of V_t/V_s were made for room temperature and 272°C. The calculated γ_b are given in Table III, where the combined effect

TABLE III

Estimate of Basal Shear Strain in the Twinned Volume

Temperature	σ_{\max} , psi	σ_b , psi	$\left(\frac{V_t}{V_s}\right)$	E, psi	γ_b , %
Room temperature	53.7×10^3	3×10^3	0.01	5.77×10^6	1664
272°C	11.5×10^3	3×10^3	0.10	4.85×10^6	9.1

(from raising temperature) of lowering σ_{\max} and increasing V_t/V_s is seen to be a reduction in γ_b by at least 2 orders of magnitude. Before shear strains of 1000% or more would be accommodated under such high loading rates, fracture could well occur. In support of large shear strains rapidly introduced, there is the extensive recrystallization of twinned material (Fig. 6), even in short time at room temperature, which indicates adiabatic deformation. Upon heating the entire crystal, elastic strain-energy storage is reduced and the twinned volume increased, with the effect that eventually basal slip may lead to work softening but not fracture.

In c-axis compression of single crystals, the transition range begins not far above 100°C. In compression perpendicular to the c-axis, crystals are reasonably ductile even at room temperature, although cracking is more obvious in the $[10\bar{1}0]$ case, which is broadly consistent with Eq. 3. Yet in a diffusely textured polycrystalline material, the transition temperature is nearer to 200°C. Perhaps the reason is that many grains in an aggregate must be more favorably oriented for basal slip than for either of these special modes of deformation, and in those grains shape change is still restricted by a shortage of independent shears. Even if five such shears can be produced in a grain, they must operate together for accommodating an arbitrary strain state. At high enough temperature, $\Delta\sigma$ in Fig. 9 practically vanishes and all grains acquire the freedom to take any shape.

The effect of certain alloying elements seems to be like that of temperature.²⁴ In particular, calcium, zirconium, thorium and/or rare

earth additions allow magnesium to be cold rolled. In terms of what has been said, the reason would involve some combination of reduced σ_{\max} , perhaps increased σ_b , and enlargement in V_t/V_s .

SUMMARY AND CONCLUSIONS

In magnesium crystals unfavorably oriented for basal slip, more or less extensive twinning occurs on $\{10\bar{1}1\}$, $\{10\bar{1}2\}$, and $\{10\bar{1}3\}$ planes. Large strains along the c-axis are only possible by operation of a double twinning mechanism -- $\{10\bar{1}1\}$ twinning followed by $\{10\bar{1}2\}$ -- and basal shear within the doubly twinned volume.

Enough independent shears for arbitrary shape change can be obtained through double twinning. However, fracture is a possible result of localized unloading from the high level of stress for initiating twinning to the much lower level for basal shear in a twin. It has been argued that ductility is achieved by raising temperature because the stress difference is lowered and the twin volume, in which elastic strain energy is dissipated on unloading, is increased.

There is no critical resolved shear stress law for $\{10\bar{1}1\}$ twinning. That has been attributed to the influence of local stress concentration at the twin site from prior intersecting shear. The suggestion is made that the strong temperature dependence of the stress for $\{10\bar{1}1\}$ twinning, whatever its absolute value, reflects the temperature dependence of the preliminary nonbasal slip.

REFERENCES

1. E. Schmid, Z. Elektrochem. 37, 447 (1931).
2. A. Beck, The Technology of Magnesium and its Alloys, p. 22, Hughes, London (1940).
3. R. von Mises, Z. angew. Math. Mech. 8, 161 (1928).
4. G. W. Groves and A. Kelley, Phil. Mag. 8, 887 (1963).
5. T. Ernst and F. Laves, Z. Metallk. 40, 1 (1949).
6. S. L. Couling, J. F. Pashak, and L. Sturkey, Trans. ASM 51, 94 (1959).
7. R. E. Reed-Hill, Trans. AIME 218, 554 (1960).
8. C. S. Roberts, Magnesium and Its Alloys, p. 94, Wiley and Sons, New York (1960).
9. I. L. Dillamore and W. T. Roberts, Met. Rev. 10, 271 (1965).
10. E. Rabinowicz, Friction and Wear of Materials, p. 218, Wiley and Sons, New York (1965).
11. J. M. Alexander, J. Mech. Phys. Solid 3, 233 (1955).
12. A. M. Montgomery, Metals Handbook, p. 1010, ASM, Cleveland (1948).
13. S. L. Couling and G. W. Pearsall, Trans. AIME 209, 939 (1957).
14. C. S. Barrett, Structure of Metals, p. 40, McGraw-Hill, New York (1952).
15. H. Conrad and W. D. Robertson, Trans. AIME 209, 503 (1957).
16. R. E. Reed-Hill and W. D. Robertson, Trans. AIME 209, 939 (1957).
17. R. E. Reed-Hill and W. D. Robertson, Trans. AIME 212, 256 (1958).
18. E. Schmid and W. Boas, Plasticity of Crystals, Hughes, London (1950).
19. P. W. Bakarian and C. H. Mathewson, Trans. AIME 152, 226 (1943).

20. P. Ward Flynn, J. Mott, and J. E. Dorn, Trans. AIME 221, 1148 (1961).
21. R. L. Bell and R. W. Cahn, Proc. Roy. Soc. A239, 494 (1957).
22. P. B. Price, J. Appl. Phys. 32, 1750 (1961).
23. P. Pointu, P. Azou and P. Bastien, C. R. Acad. Sci., Paris 252,
24. J. C. Mac Donald, Trans. AIME 212, 45 (1958).

APPENDIX 1

EXPERIMENTAL DETAILS

I. Crystal Growth

By spectrographic analysis, the sublimed magnesium contained in weight percent: <0.001 Al, <0.01 Ca, <0.001 Cu, <0.0007 Fe, <0.001 Mn, <0.0005 Ni, <0.003 Pb, <0.001 Si, <0.01 Sn, <0.001 Zn. The material was rolled at about 400°C into strips approximately $3/8$ -in. in thickness. The rolled strip was first straightened by applying about 3% tensile strain in an Instron machine, and then machined into blanks $1/4 \times 1/8 \times 5$ in. The machined blanks were abraded on 600 grit silicon carbide paper, and given a light chemical polish in 25% hydrochloric acid. Blanks with more than 0.0002 in overall taper were rejected.

Next, a previously grown seed crystal was Heliarc welded (with argon) to the blank. To check the orientation of the seed, the blank and seed crystal were placed in a jig designed to hold the blank perpendicular to an x-ray beam and a back-reflection Laue photograph was taken of the seed. If any adjustment in orientation of the seed crystal was necessary, a small notch was carefully cut with a jeweler's saw into the end of the blank just above the weld and the necessary rotation made. The seed was X-rayed again and, if necessary, the procedure was repeated.

The blank and seed were placed in a capped, split, graphite tube (1 in. x 8 in.), and 100 mesh graphite powder was gently but firmly

packed around the blank and seed to form a "soft" mold. Care was taken to degas the tube and powder at 1000°C under vacuum.

The blank, seed, and mold were placed in a horizontal gradient furnace, and after melting into the seed, a crystal was grown at a rate of 1 cm./hr. under an atmosphere of anhydrous sulphur dioxide. The sulphur dioxide eliminated evaporation and sublimation which occurred under a helium atmosphere.

After growth, the split mold was separated and the crystal gently removed from the packed graphite powder. After a light etch in 25% hydrochloric acid, the crystal was checked for stray grains and the final orientation determined by back-reflection Laue photographs. All crystals tested were free of stray grains and showed sharp Laue spots with no asterism.

II. Testing

Small test pieces ($1/8 \times 1/4 \times 5/8$ in.) were cut from the crystals with a thread acid saw,* using 50% hydrochloric acid, degreased with trichloroethylene, and lubricated with a colloidal molybdenum disulphide spray. The specimen was inserted in a similarly lubricated adjustable vise-like channel (Fig. 1A). The vise was constructed of surface ground air hardened steel (Carpenter 610) and the adjustable

* R. Maddin and W. R. Asher, Review of Scientific Instruments 21, 881 (1950).

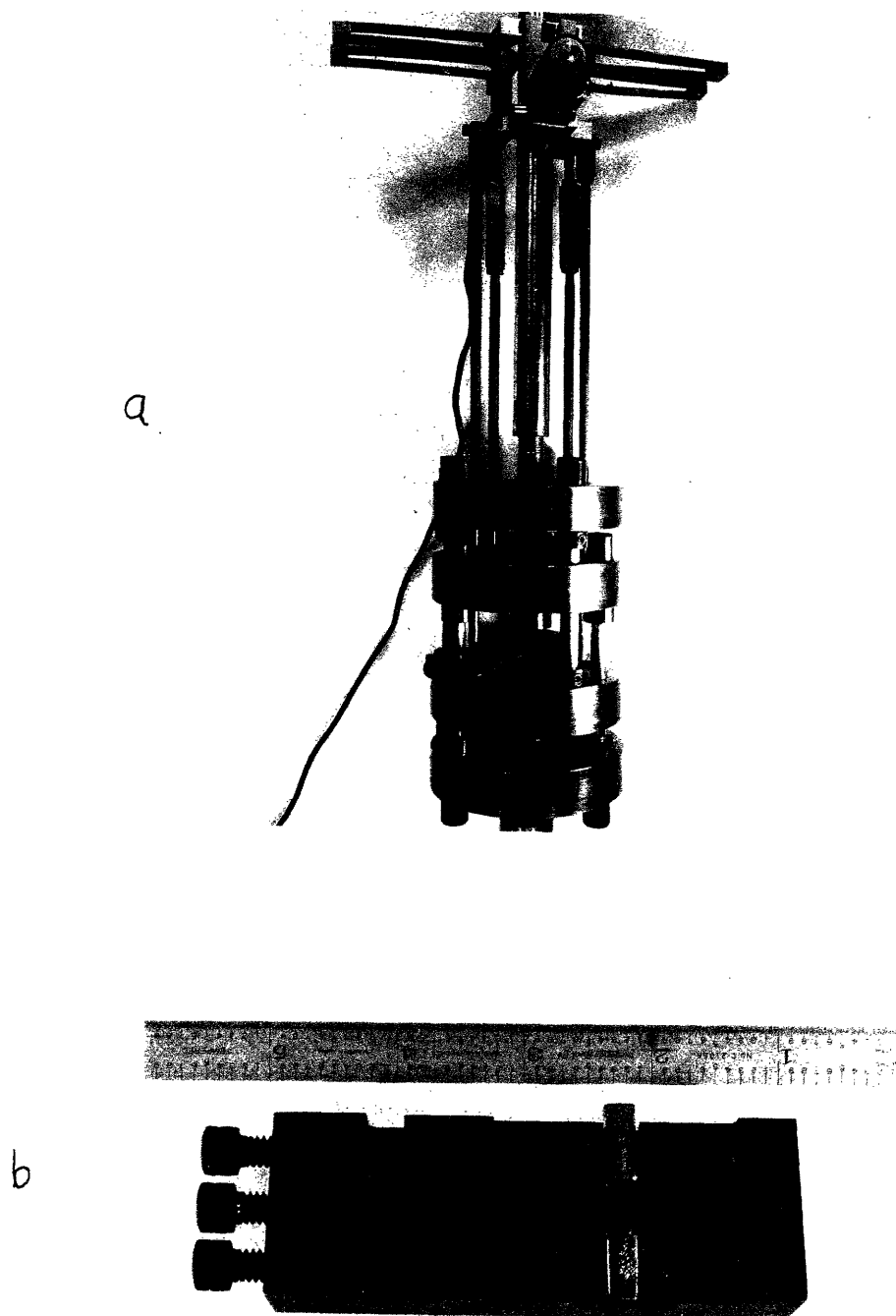


Fig. 1A. Experimental Apparatus

- (a) Compression fixture and extensometer with channel, specimen and indenter in place.
- (b) Adjustable channel with specimen and indenter inserted.

jaw was supported by 3-1/4 x 20 hardened cap screws. The vise jaw was then brought up finger tight on an indenter which was larger than the crystal by no more than 0.0005 in. The crystal, indenter, and channel were placed in a compression fixture (Fig. 1A) consisting of two interpenetrating cages. The top and bottom of each cage consists of 1 x 5 inch discs supported by three 3/8 in. diameter polished, hardened steel rods. When the two cages were pulled apart by the Instron machine during the test, the two inner discs are pulled together thus compressing the crystal. To assure axial loading the fixture was adjusted so that the discs were parallel within 0.01 degree.

To allow continuous record of displacement a Wiedeman microformer (linear variable differential transformer) was coupled to the inner discs with long brass rods. By adjusting the length of the rods with turn-buckles, the microformer could be kept in the linear region. Before each test the microformer was calibrated by displacing the fixture in the Instron machine a known amount (usually half the linear range of the microformer, 0.020 in.) by running at a fixed speed for a given time and measuring the resulting displacement on the X-Y chart record. The procedure was repeated before and after each series of tests as was the standard calibration of the Instron load measuring system.

During testing at elevated temperatures, the fixture was immersed in silicone oil (Dow Corning 710) heated with two 1-kilowatt immersion heaters controlled by a Bristol Dynamaster recorder. Temperature was monitored with a iron-constantan thermocouple pressed against the indenter.

An initial region of upward curvature was present in all stress-strain curves, and was not reproducible. Several factors could contribute to the region. The first is extrusion of lubricant layers, which was eliminated by spraying a light layer (about 10 microns) of molybdenum disulphide. The use of 3 mil teflon film, which has a somewhat lower coefficient of friction than the spray used, increased the extent of curvature. Second, any taper in the specimen would contribute to the extent of curvature and specimens were machined to insure less than 0.0002 in. taper, and the alignment of platens was adjusted to within 0.01° . The most difficult problem, however, was the rough surface produced by crystal growth. By careful mechanical polishing, the crystal surface could be smoothed and the low stress region virtually eliminated (Fig. 1B). Significantly, if the stress-strain curve for the rough (as grown) crystal was translated horizontally, it coincided with the stress strain curve for the polished crystal. Also, a crystal was deliberately roughened with a coarse file and, upon testing, the extent of curvature was found to increase. Further an estimate of the average height of the growth asperities was 1 to 1.5 mils, made by abrading the specimen on 600 paper until a uniformly bright surface was obtained and measuring the change in dimension with a micrometer. The extent of curvature was generally 1 to 3%, and it is consistent with the strain required to flatten the asperities of the top and bottom surfaces.

Since the initial curvature did not affect the reproducibility and since handling during polishing would have damaged the very soft crystals

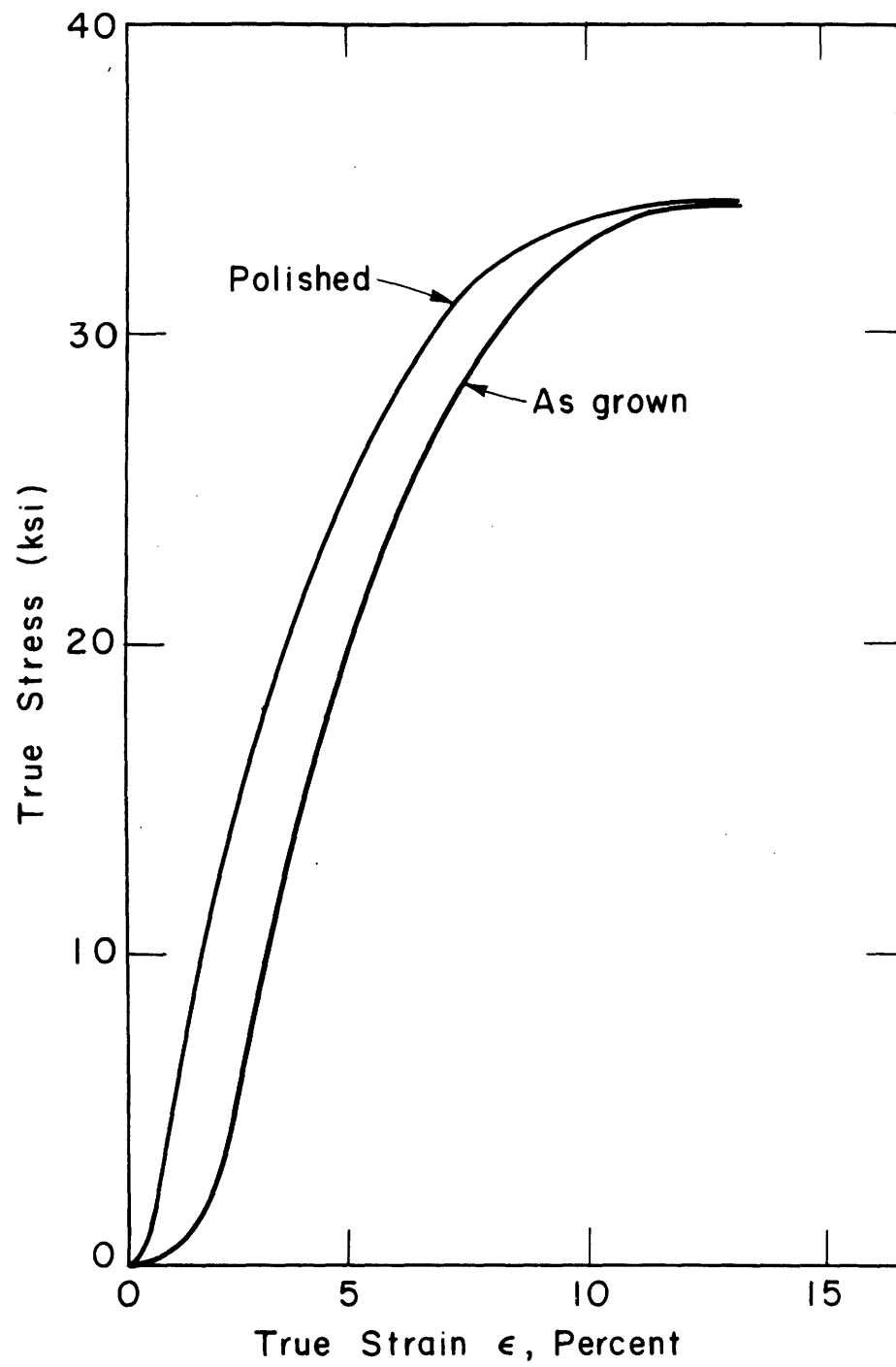


Fig. 1B. True-stress:true-strain Plane-strain Compression Curves for Single Crystals of Differing Surface Roughness.

(yield stress as low as 140 psi in some directions), no effort other than a light chemical polish was made to reduce roughness. Heavy chemical polishing produced smooth but rounded surfaces, and so actually increased the extent of curvature.

APPENDIX 2

CALCULATION OF LINEAR HARDENING RATE
DUE TO ELASTIC EFFECTS IN CHANNEL

The initial slope of the stress strain curve can be estimated by assuming that the lateral strain ϵ_r due to $\{10\bar{1}2\}$ twinning is resisted by a linear elastic stress σ_r from the channel wall and simultaneously requiring that the resolved shear stress $\tau_{\{10\bar{1}2\} \langle 10\bar{1} \rangle}$ on the $\{10\bar{1}2\}$ plane be the current value required for twinning.

The elastic reaction stress for channel of transverse stiffness K is

$$\sigma_r = - K \epsilon_r$$

$\gamma_{\{10\bar{1}2\} \langle 10\bar{1} \rangle}$ related to the normal applied strain ϵ_a and the lateral strain ϵ_r :

$$\gamma_{\{10\bar{1}2\} \langle 10\bar{1} \rangle} = \frac{\epsilon_a}{m_a} = \frac{\epsilon_r}{m_r}$$

where m_a and m_r are the Schmid factors for $\{10\bar{1}2\} \langle 10\bar{1} \rangle$ twinning in the a and r directions.

Thus the reaction stress in terms of the applied strain ϵ_a is

$$\sigma_r = - K \left(\frac{m_r}{m_a} \right) \epsilon_a \quad (1)$$

The shear stress for twinning $\tau_{\{10\bar{1}2\} \langle 10\bar{1}1 \rangle}$ is related to the applied and reaction stresses by (see Appendix 3 for details)

$$\tau_{\{10\bar{1}2\} \langle 10\bar{1}1 \rangle} = m_a \sigma_a + m_r \sigma_r \quad (2)$$

If Equations (1) and (2) are solved the following is obtained:

$$\sigma_a = K \left(\frac{m_r}{m_a} \right)^2 \epsilon_a + \frac{\tau_{\{10\bar{1}2\} \langle 10\bar{1}1 \rangle}}{m_a} \quad (3)$$

Differentiating with respect to ϵ_a to obtain the hardening rate $\theta = \frac{d\sigma}{d\epsilon}$:

$$\theta = \frac{d\sigma_a}{d\epsilon_a} = K \left(\frac{m_r}{m_a} \right)^2 + \frac{1}{m_a} \frac{d\tau}{d\gamma} \left\{ 10\bar{1}2 \right\} \langle 10\bar{1}1 \rangle$$

The hardening rate θ is composed to two additive terms: the first depends only on the transverse stiffness of the channel and the orientation of the twin system; the second depends on the fundamental work hardening rate of the twinning process $\frac{d\tau}{d\gamma}$. Since experimentally

$\sim \frac{1}{10} E$ and $\frac{d\tau}{d\gamma} \left\{ 10\bar{1}2 \right\} \langle 10\bar{1}1 \rangle \sim \frac{1}{100} E$,
the contribution of

$$\frac{d\tau}{d\gamma} \left\{ 10\bar{1}2 \right\} \langle 10\bar{1}1 \rangle$$

can be neglected and

$$\theta \approx K \left(\frac{m_r}{m_a} \right)^2$$

For the case of compression along $[10\bar{1}0]$ with constraint along $[0001]$,
 $m_a = \cos 46.85 \sin 43.15 = 0.499$ and $m = -\cos 43.15 \cos 46.85 = -0.499$

$$\odot [10\bar{1}0] \approx K$$

For the other case, compression along $[1\bar{2}10]$ with constraint along $[0001]$, $m_a = 0.75 \cos 43.15 \cos 46.85 = 0.374$, $m_r = -\cos 43.15 \cos 46.85 = -0.499$

$$\odot [1\bar{2}10] = 0.562 K$$

The ratio $\frac{\odot [10\bar{1}0]}{\odot [1\bar{2}10]} = 1.78$, which is nearly what is observed (Table II).

APPENDIX 3

CALCULATION OF RESOLVED SHEAR STRESS
FOR $\{10\bar{1}1\} \langle 10\bar{1}2 \rangle$ TWINNING

A resolved shear stress for $\{10\bar{1}1\}$ twinning can be calculated by assuming that the applied and reactive stresses must satisfy the shear stress requirements for twinning on both $\{10\bar{1}2\}$ and $\{10\bar{1}1\}$ simultaneously.

The shear stress τ_{ns} on a plane with normal \bar{n} and in a direction \bar{s} under biaxial load from the applied and reaction stresses σ_a and σ_r is given by:

$$\tau_{ns} = l_{na} l_{sa} \sigma_a + l_{nr} l_{sr} \sigma_r$$

where l_{ij} is the direction cosine between i and j axis.

Specifically, for a crystal stresses along the $[10\bar{1}0]$ direction by σ_a and restrained along the $[000\bar{1}]$ direction by σ_r , the shear stress on the $(10\bar{1}2)$ twin system is:

$$\begin{aligned} \tau_{(10\bar{1}2)[10\bar{1}1]} &= + \cos 46.85 \cos 43.15 \sigma_a - \cos 43.15 \cos 46.85 \sigma_r \\ &= 0.499 (\sigma_a - \sigma_r) \end{aligned}$$

Similarly for $(01\bar{1}1)$ twin in the same crystal:

$$\begin{aligned} \tau_{(01\bar{1}1)[01\bar{1}2]} &= \cos 28.1 \cos 61.9 \sigma_r - 1/4 \cos 61.9 \cos 28.1 \sigma_a \\ &= 0.416 \sigma_r - 0.104 \sigma_a \end{aligned}$$

Solving the two equations for the shear stress in terms of the applied σ_a , the following is obtained.

$$\tau_{(01\bar{1}1)[01\bar{1}2]} = 0.312 \sigma_a - 0.834 \tau_{(10\bar{1}2)[10\bar{1}1]}$$

Since experimentally $\tau_{(10\bar{1}2)[10\bar{1}1]} \ll \sigma_a$,

$$\tau_{(01\bar{1}1)[01\bar{1}2]} \approx 0.312 \sigma_a$$

The approximation represents the highest value of $\tau_{(01\bar{1}1)[01\bar{1}2]}$ since increasing $\tau_{(10\bar{1}2)}$ tends to decrease the shear stress resolved on the $(01\bar{1}1)$ twin system.

For the case of a crystal compressed along $[1\bar{2}10]$ and restrained along $[0001]$:

$$\begin{aligned} \tau_{(10\bar{1}2)[10\bar{1}1]} &= 3/4 \cos 43.15 \cos 46.85 \sigma_a - \cos 43.15 \cos 46.85 \sigma_r \\ &= 0.374 \sigma_a - 0.499 \sigma_r \end{aligned}$$

$$\begin{aligned} \tau_{(01\bar{1}1)[01\bar{1}2]} &= 0. \sigma_a + \cos 61.9 \cos 28.1 \sigma_r \\ &= 0.416 \sigma_r \\ &= 0.312 \tau_a - 0.834 \tau_{(10\bar{1}2)[10\bar{1}1]} \end{aligned}$$

which is identical to the previous result.

APPENDIX 4

PROOF THAT A $(01\bar{1})$ PLANE IN THE MATRIX IS NEARLY
PARALLEL TO A $\{01\bar{1}\}$ PLANE WITHIN A $(10\bar{1}2)$ TWIN

For the particular case of a $(01\bar{1})$ twin impinging on a $(10\bar{1}2)$ twin, the following angular relationships apply:

1. The angle b between the $[0001]$ in the matrix and the $(01\bar{1})$ pole in the matrix is 61.9° .
2. The angle c between the $[0001]$ in the matrix and the $[0001]$ in the $(10\bar{1}2)$ twin is 86.3° .
3. The angle A between the two great circles connecting $[0001]$ in the matrix with the $(01\bar{1})$ pole, and the $[0001]$ in the matrix with the $[0001]$ in the $(10\bar{1}2)$ twin is 60° .
4. The three poles in question, $[0001]$ in the matrix, $[0001]$ in the $(10\bar{1}2)$ twin, and the pole of $(01\bar{1})$ in the matrix, form on the reference sphere a spherical triangle of sides $b = 61.9^\circ$, $c = 86.3^\circ$, and included angle $A = 60^\circ$. The third side a , and the other included angles B and C are unknown.

If the $(01\bar{1})$ plane in the matrix is parallel to a $\{01\bar{1}\}$ plane in the $(10\bar{1}2)$ twin, the unknown side a between the pole of $(01\bar{1})$ in the matrix and $[0001]$ in the $(10\bar{1}2)$ twin ought to equal 61.9° .

The following relation holds for all spherical triangles:

$$\cos a = \cos b \cos c + \sin b \sin c \cos A$$

inserting the above values,

$$\cos a = \cos 61.9^\circ \cos 86.3^\circ + \sin 61.9^\circ \sin 86.3^\circ \cos 60^\circ$$

$$\cos a = (.471) (.0645) + (.998) (.8821) (.5)$$

$$= 0.0304 + .4401$$

$$= 0.4705$$

or

$$a = 61.93^\circ$$

which is nearly the value expected.

The final requirement is that the included angle B between the sides a and c ought to be 60° , corresponding to the angle between the two $\langle 11\bar{2}0 \rangle$ zones in the $(10\bar{1}2)$ twin.

The relationship between the included angle and opposite side for any spherical triangle is

$$\frac{\sin A}{\sin a} = \frac{\sin B}{\sin b}$$

For the case in question

$$\frac{\sin 60^\circ}{\sin 61.9^\circ} = \frac{\sin B}{\sin 61.9^\circ}$$

thus, $B = 60^\circ$, which again is the required angle.

Therefore, a $(01\bar{1}1)$ in the matrix is parallel within 0.1° of a $\{01\bar{1}1\}$ plane in a $(10\bar{1}2)$ twin.

SUGGESTIONS FOR FUTURE RESEARCH

1. Other HCP Metals

Beryllium is generally brittle. Titanium and zirconium are much more ductile, although in both fracture remains a problem which can limit their processing. Recently, fracture in titanium was related to $\{11\bar{2}2\}$ twins, either by twin-matrix separation or by cracks formed through secondary twinning.* Similarly, cleavage cracks have been found in beryllium at the $\{10\bar{1}2\}$ twin-matrix interface.** The factors which control twinning in hcp metals probably also control fracture. Therefore, the effect of crystal orientation, temperature, alloying content and strain rate on the various twin systems ought to be carefully investigated along the lines of the present work.

2. Effect of Alloying

The similarity between the effect of temperature and the effect of certain alloying additions (calcium, thorium, zirconium and the rare earths) has been pointed out and should be studied by tests on alloy

* H. J. Burrier, Jr., M. F. Amateau and E. A. Steigerwald, Air Force Materials Laboratory Technical Report AFML-TR-65-239, July 1965.

** G. L. Tuer and A. R. Kaufmann, The Metal Beryllium, p. 372, ASM, Cleveland (1955).

single crystals. Specifically, c-axis compression experiments as a function of alloy content could be made to determine if the stress for $\{10\bar{1}\}$ twinning does decrease with alloying. If it does, the reason may be that the stress for nonbasal slip is lowered, and that should be studied by tension test perpendicular to the $[0001]$ accompanied by careful slip-trace studies or electron microscopy.

3. Determination of Nonbasal Slip Direction

Since slip out of the basal plane might only be a prelude to twinning and therefore, its extent limited, it may be difficult to observe by conventional microscopy. A method for detecting a possible nonbasal Burgers vector is to observe by transmission electron microscopy a thin foil containing the $[0001]$ direction in the plane of the foil. Dislocations in the (0001) plane will be foreshortened in that view and by a suitable choice of diffraction conditions all dislocations with Burgers vectors in the basal plane can be eliminated. Thus only dislocations associated with slip in a direction out of the basal plane will be visible.

Observations could be made on a number of samples compressed to various strains along the c-axis. A further variation would be to grow, by vapor deposition, thin magnesium foils and pull them parallel to the basal plane in the microscope, and try to observe directly the events which precede twinning.

4. Effect of $\{10\bar{1}2\}$ Twinning During Unloading

Although $\{10\bar{1}2\}$ twinning occurred under macroscopic residual stresses in the present tests, it might also occur during load-unload tension tests of polycrystalline h.c.p. metals due to microscopic residual stresses set up between neighboring grains. If so, a difference between continuous tension tests and load-unload tests might appear in the stress-strain curves and the ratio of plastic width to thickness strains.

BIOGRAPHICAL NOTE

Bud Caesar Wonsiewicz, eldest son of Mr. and Mr. C. B. Wonsiewicz of Allentown, Pennsylvania, was born on August 23, 1941 in Buffalo, New York. During the period 1959 - 1963 he attended Massachusetts Institute of Technology, and received a Bachelor of Science in Metallurgy in 1963. That same year he entered graduate school as a research assistant in the Department of Metallurgy at M.I.T.

In June, 1963 he married Marie A. Gallagher. They are the parents of two children, Susan, age 1-1/2 years, and Thomas Michael, age 8 weeks.

He has been elected to Sigma Xi, and is a member of the American Society for Metals, and the American Institute of Mining, Metallurgical, and Petroleum Engineers.